ERDC /CHL TR-18-4

US Army Corps
of Engineers®
Engineer Research and
Development Center

ERDC
INNOVATIVE SOLUTIONS
for a safer, better world

Silver Creek: A Study of Stream Velocities and Erosion along the Ohio River near Clarksville, Indiana

McAlpine Lock and Dam Numerical Model

Keaton E. Jones, David D. Abraham, Gary L. Bell, and Nate D. Clifton

April 2018

Coastal and Hydraulics Laboratory

The U.S. Army Engineer Research and Development Center (ERDC) solves the nation's toughest engineering and environmental challenges. ERDC develops innovative solutions in civil and military engineering, geospatial sciences, water resources, and environmental sciences for the Army, the Department of Defense, civilian agencies, and our nation's public good. Find out more at www.erdc.usace.army.mil.

To search for other technical reports published by ERDC, visit the ERDC online library at http://acwc.sdp.sirsi.net/client/default.

ERDC/CHL TR-18-4
April 2018

Silver Creek: A Study of Stream Velocities and Erosion along the Ohio River near Clarksville, Indiana

McAlpine Lock and Dam Numerical Model

Keaton E. Jones, David D. Abraham, Gary L. Bell,
and Nate D. Clifton

Coastal and Hydraulics Laboratory
U.S. Army Engineer Research and Development Center
3909 Halls Ferry Rd
Vicksburg, MS 39180-6199

Final report

Prepared for U.S. Army Corps of Engineers, Louisville District
Mazzoli Federal Building
600 Dr. Martin Luther King Jr. Place
Louisville, KY 40201-0059

Under Project No. 455010, "The Silver Creek Floodplain Management Services Project: A Study of Stream Velocities and Erosion along the Ohio River near Clarksville, Indiana"

Abstract

The River Engineering Branch of the Coastal and Hydraulics Laboratory conducted a two-dimensional numerical model investigation of the Ohio River immediately downstream of McAlpine Lock and Dam. The right bank between river mile 605.5 and 606.5 (opposite the dam's downstream set of tainter gates) has historically experienced stability issues. Conditions on the bank, when observed through aerial imagery, appear most severe when the dam is releasing all or most flow through the downstream (lower) set of tainter gates. Releasing all flow through the downstream gates occurs only at lower flow rates, but this study determined that standard high-flow conditions create higher velocities in the problem area than these observed low-flow conditions. The representative high-flow event was then used to test the capability of structural alternatives to reduce velocities in the area of concern. Plans consisting of small emergent dikes placed along the shoreline were able to reduce the velocities significantly and could be a feasible alternative to help protect the bankline.

Contents

Figures and Tables

Figures

Tables

Preface

This study was conducted for the U.S. Army Corps of Engineers, Louisville District, under Project No. 455010, "The Silver Creek Floodplain Management Services Project: A Study of Stream Velocities and Erosion along the Ohio River near Clarksville, Indiana." The technical monitor was Mr. Tracy Keel.

The work was performed by the River Engineering Branch (CEERD-HFR) of the Flood and Storm Protection Division (CEERD-HF), U.S. Army Engineer Research and Development Center, Coastal and Hydraulics Laboratory (ERDC-CHL). At the time of publication, Mr. Keith W. Flowers was Chief, CEERD-HF-R; Dr. Cary A. Talbot was Chief, CEERD-HF. The Acting Deputy Director of ERDC-CHL was Dr. Jackie S. Pettway, and the Acting Director was Mr. Jeffrey R. Eckstein.

COL Bryan S. Green was the Commander of ERDC, and Dr. David Pittman was the Director.

Unit Conversion Factors

Multiply	By	To Obtain
acres	4,046.873	square meters
cubic yards	0.7645549	cubic meters
feet	0.3048	meters
miles (U.S. statute)	1,609.347	meters
square feet	0.09290304	square meters

1 Introduction

1.1 Objective

The River Engineering Branch of the U.S. Army Research and Development Center (ERDC), Coastal and Hydraulics Laboratory (CHL), conducted a numerical hydraulic and sediment model for the U.S. Army Corps of Engineers (USACE), Louisville District, to examine the prudent use and best management practices of the Ohio River floodplain near the Falls of the Ohio and the McAlpine Lock and Dam. The study was initiated to determine the causative factors of scour on the north shore of the Ohio River between river miles (RM) 605.5 and 606.5 at the town of Clarksville, IN, across the river from Louisville, KY. In addition, the study evaluated possible alternatives to eliminate or reduce the scour. A two-dimensional (2D) Adaptive Hydraulics (AdH) sediment model was developed, and existing conditions were tested to determine what flow conditions create the most flow impingement on the bank in the area of study. Once the worst conditions were determined, five structural alternatives were tested to determine their impacts during the worst operational scenario.

1.2 Background

The location of the erosion problem area is just downstream of the McAlpine Lock and Dam. McAlpine Lock and Dam is located at RM 604.5 of the Ohio River at Louisville, KY. McAlpine Dam has three release locations including a hydropower facility and two sets of tainter gates. These tainter gates, the most upstream (upper) and downstream (lower), are a critical aspect of this study and are mapped in Figure 1 along with the problem area.

Figure 1. Study site.

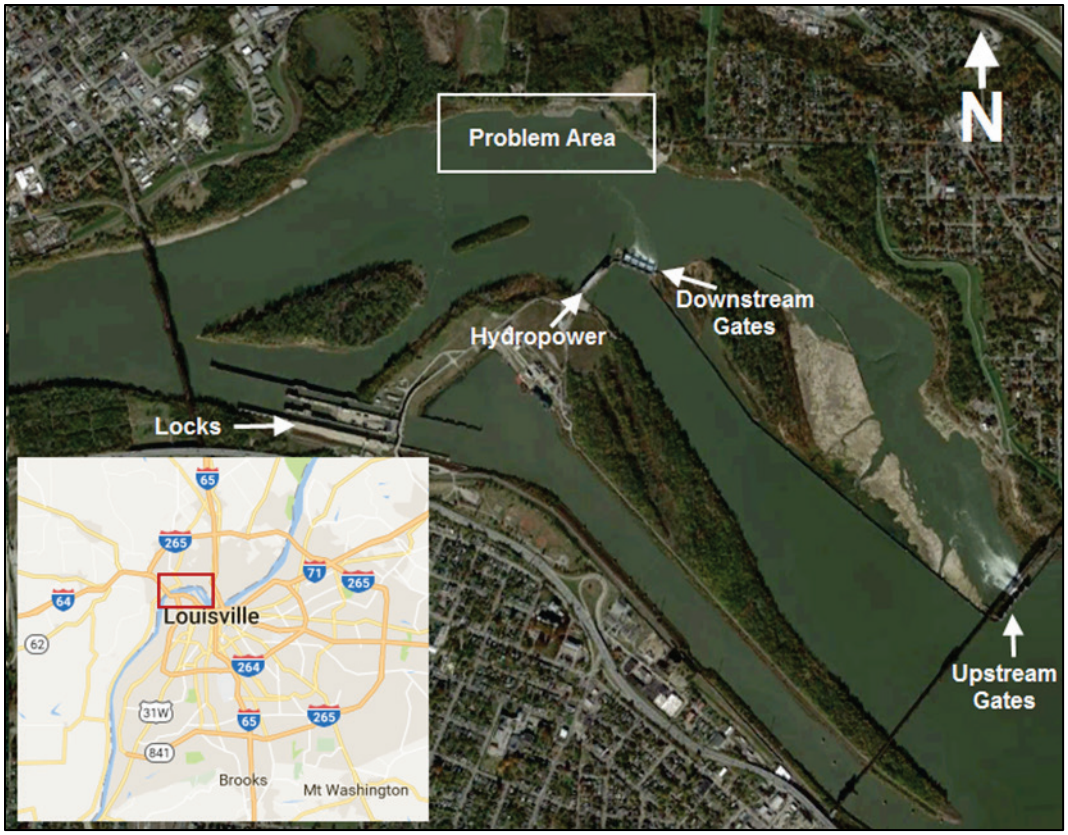

This study resulted from the 2015 report *Ohio River Shoreline, McAlpine Locks and Dam Caving Bank Condition, Clarksville, Indiana Followup Assessment Report*, by the USACE Louisville District (USACE 2015). The report includes findings from an investigation of bank failure and erosion issues on the north shore of the Ohio River between RM 605.5 and 606.5. The report presents a summary of prior studies, reports, and projects dating back to 1973 that address the erosion. Figure 2 is an image from a 2004 bank erosion event that was included in the report. The previous report concludes that the shoreline failure is likely a combination of geotechnical and hydraulic issues and that potential measures to address the problem include construction of bank revetment, shoreline walls, or dike jetties.

Figure 2. 2004 Bank erosion in problem area.

1.3 Approach

The modeling approach is addressed in Chapter 2 Model Development, Section 2.1 Approach.

2 Model Development

2.1 Approach

The investigation was performed using the AdH numerical model. AdH is a multi-physics, finite element code capable of automatically refining the unstructured computational mesh when necessary to resolve gradients in the flow field (ERDC CHL 2017). The AdH model used in this study was conducted using the 2-D depth-averaged shallow water module, which was necessary to capture the flow release of the lower tainter gates. These flows enter the main channel at a nearly 90 degree angle perpendicular to the incoming flow from the upstream gates and then turn downstream, which can be seen in Figure 1. Depending on the flow split between the upper and lower gates, the tainter gate outflow can cause flow circulations or eddies to form, which requires the use of a multi-dimensional model to simulate. A three-dimensional (3D) Navier Stokes model can resolve vertical velocities from helical flow that could occur as flow released from the lower gates turns downstream, but the model requires much more computational time and a smaller domain. AdH 2D shallow water module accounts for 3D effects of the helical flow by using a vorticity bendway correction (ERDC CHL 2017). The 2D model was chosen due to the ability to account for the vorticity and having less time and spatial constraints than the 3D model. AdH also has the ability to simulate multi-grain size sediment transport, which was implemented in this model and intended to assist in determining the causes and trends of the scour behavior observed in the field. As the study moved forward, velocity results including magnitudes and directions were determined to be the best comparison of the erosion potential at the bank.

2.2 Mesh development

The computational domain is a triangulated mesh composed of triangular elements and nodes where hydraulic computations occur. The extent of the AdH model mesh is outlined by the blue line in Figure 3 and includes the Cannelton pool of the Ohio River from the McAlpine Dam upper tainter gates at RM 604.5 to RM 627.2 where U.S. Geological Survey (USGS) gage 03294600 (Ohio River at Kosmosdale, KY) is located.

Figure 3. Mesh extents.

The mesh covers 4,665 acres and contains 44,266 nodes and 86,368 elements. The mesh consists of triangular elements composed of three nodes. Nodes are points at which computations of depth, velocity, and sediment calculations occur. Element sizes range from 200 feet (ft) in the downstream end to 20 ft in the project area of concern. The horizontal projection is State Plane Kentucky North NAD83, and the vertical projection is Ohio River Datum. The units are specified as meters in the model to allow AdH to perform sediment transport calculations, but reported hydraulic parameters have been converted to English units. The focus area is the entire mesh upstream of RM 608. Mesh bathymetry in

the focus area includes 2016 multi-beam data collected by the CHL Field Data Collection Branch. Cross-sectional data measured previously in 2009 were used downstream of the focus area. Due to bathymetry being collected during relatively low-water conditions, airborne light detection and ranging (lidar) data obtained from Indiana's online database were used to extend elevations to the mesh boundaries. Mesh elevations for the entire model domain are shown in Figure 4, and Figure 5 shows a closer view of elevations in the focus area.

Figure 4. Model elevation relative to Ohio River datum.

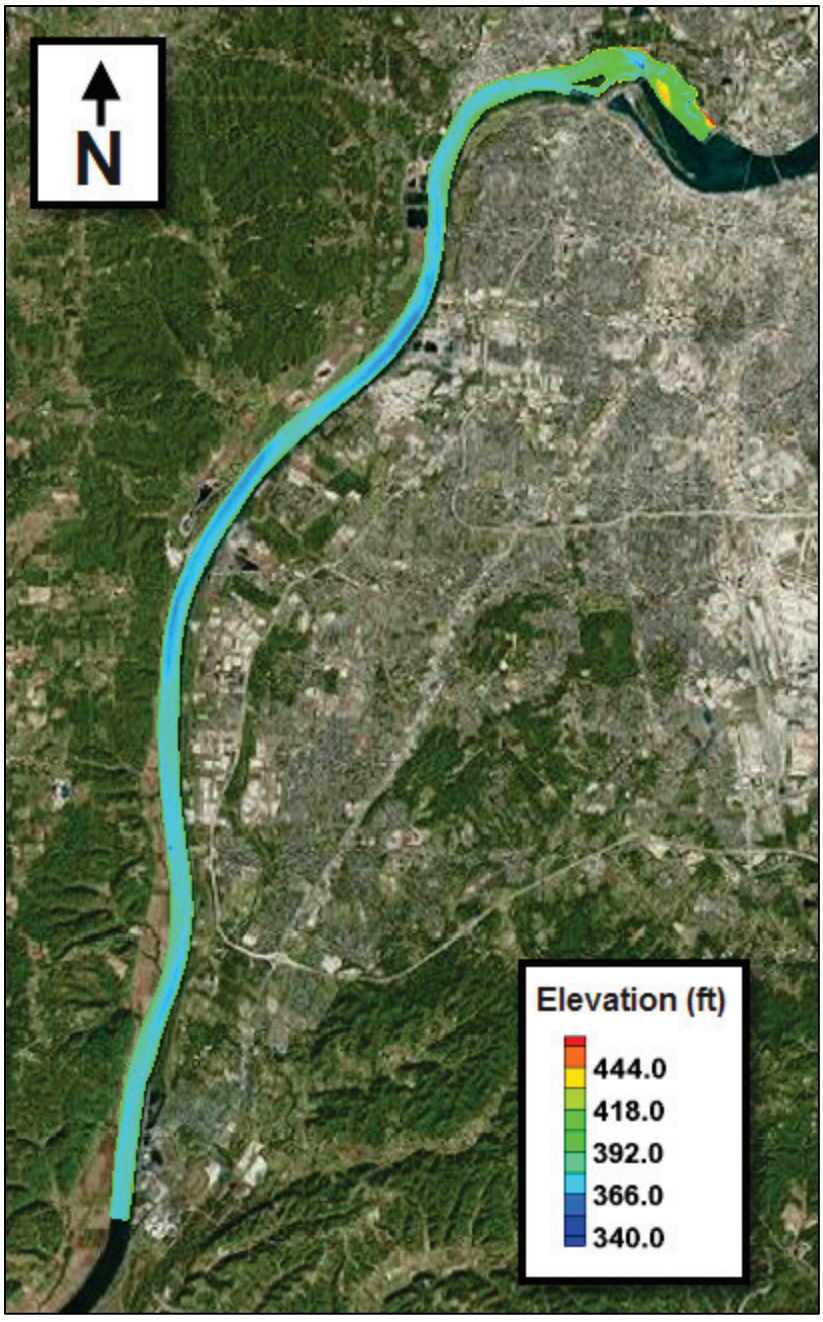

Figure 5. Model elevation in focus area relative to Ohio River datum.

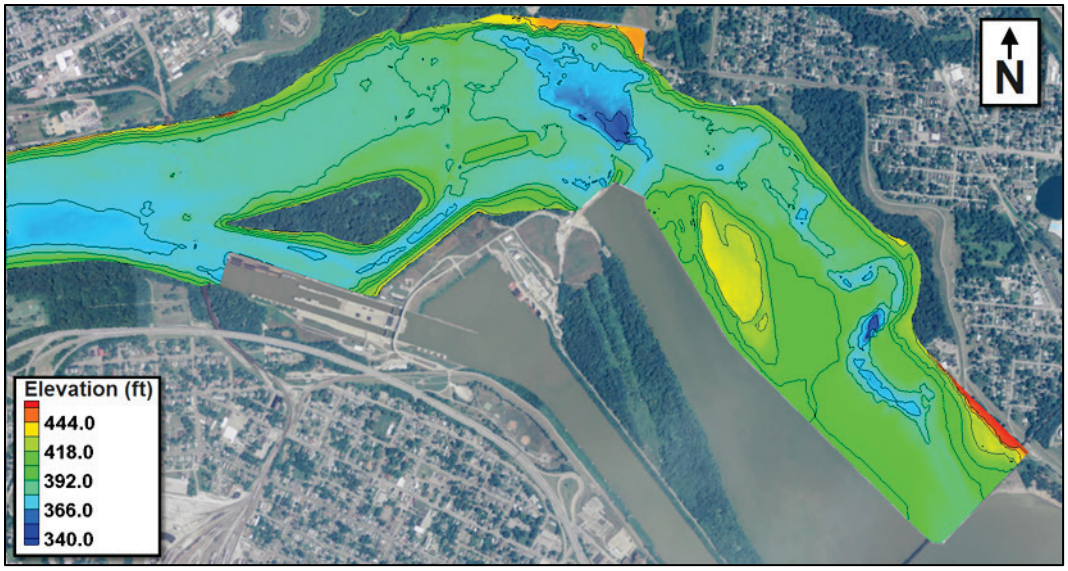

Nine different material types were assigned to the model mesh elements. Each material type is a group of elements that can be assigned different attributes that affect hydraulics and sediment calculations. In this model, each material type was assigned a friction value, bed gradation, bed layer thickness, and the ability to erode or not. Respective locations of the different material types are shown below in Figure 6. (Note: Navigation Channel material type extends to the downstream end of the mesh.)

Figure 6. Material type locations.

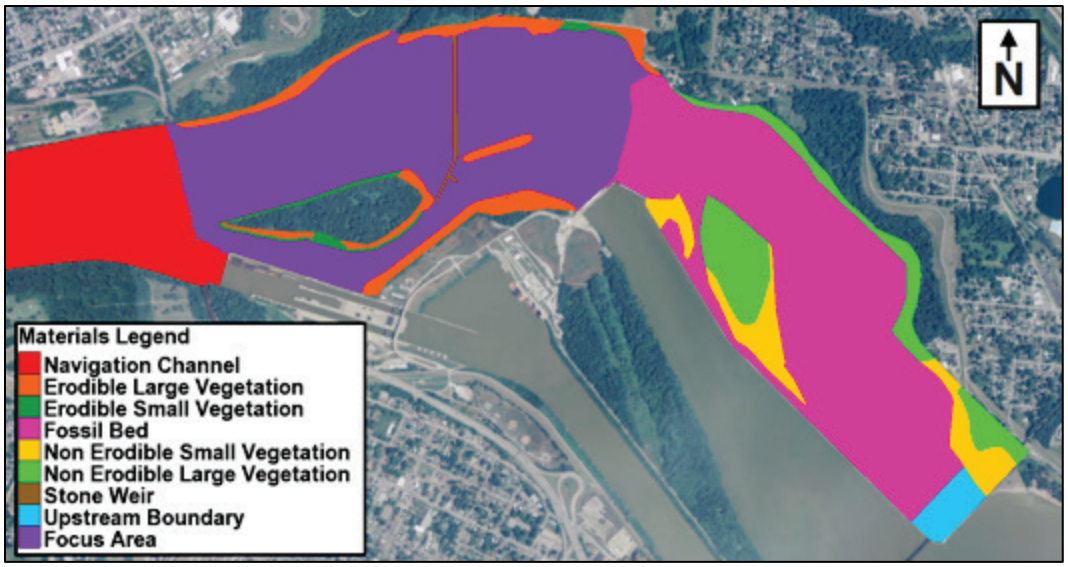

2.3 Hydraulic and sediment boundary conditions

The AdH model for this area has three controlled inflow locations and one downstream tail water control. Inflows in the model can be specified through the upstream (upper) tainter gates, downstream (lower) tainter gates, and Louisville Gas and Electric powerhouse, which are shown in Figure 7. During high water, flow will pass over the weir wall connecting the upstream and downstream tainter gates. This can be seen in the high-flow aerial image (Figure 34) in Section 4. These flows were not input over the weir wall in the model; instead, they were routed through the upstream gates. This was done to simplify the inputs, and once these extra flows reach the project area, they are expected to behave similarly whether input over the weir wall or added to the flow through the upstream gates. Also, knowing where and how much water to input over the weir would be difficult. The tail water control is located at the downstream end of the model at RM 627.2. There is an existing USGS gage at this location, so historic water surface elevations can be assigned accurately.

Figure 7. Location of discharge boundaries.

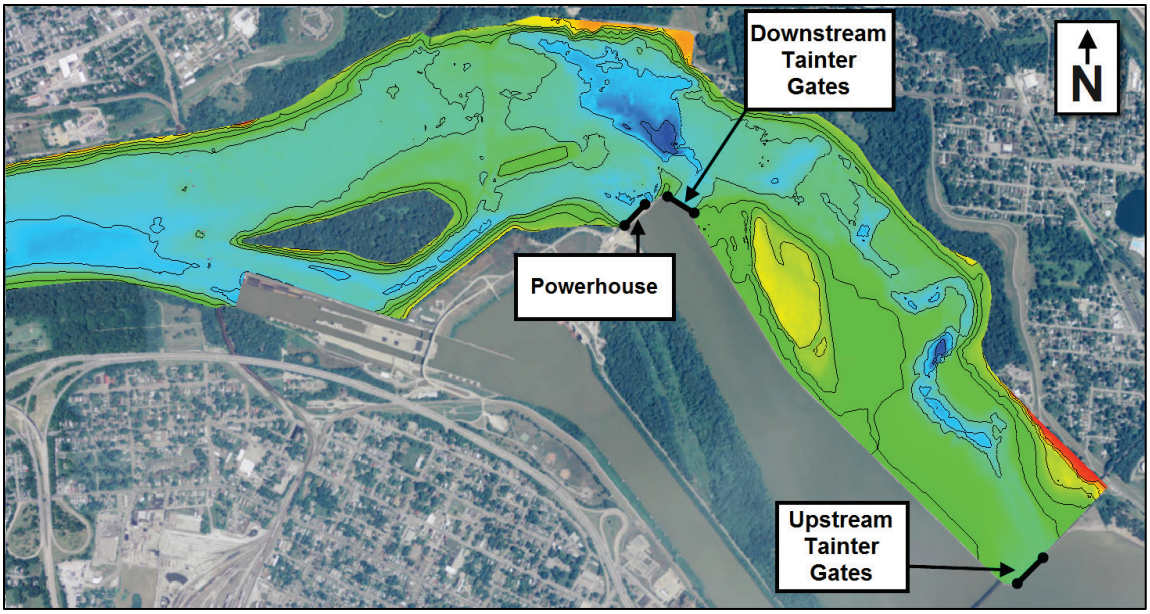

For AdH to perform sediment transport, there must be specified transport functions, sediment boundary conditions, and bed characteristics. This model uses Wright-Parker noncohesive suspended entrainment equations and the Meyer-Peter Müller bedload entrainment equations with the Wong-Parker correction (Wright and Parker 2004; Meyer-Peter and Müller 1948; Wong and Parker 2006). The model also uses the Egiazaroff

noncohesive hiding factor (Egiazaroff 1965). Bed samples were collected during the field data collection trip, which took place in July 2016, and were used to help assign starting bed gradations. Locations of samples in the project area are mapped in Figure 8. The numbers represent the river mile location, and the letters R, RC, M, LC, and L represent the relative location in the river (decending right bank, right center, middle, left center, and left bank, respectively). The label "Chute" refers to the side channel between the locks and islands, which can be seen in the figure. The grain sizes used in this model are shown below in Table 1. All nodes of a material type must be assigned the same bed characteristics including bed gradation. Realistically, the bed gradation over these large areas can be quite variable. Thus, an initialization run was performed to allow the grains to be sorted and create more realistic and spatially varying starting bed gradations and thicknesses.

The initialization run consisted of a 100-day steady flow. During the initialization run, the geometry of the model was held constant, but the sediment was allowed to move. This results in the model sorting the different grain sizes, causing armoring in higher velocity areas and fining of bed sediments in lower velocity depositional portions of the bed. For the initialization run, sediment boundary conditions included specified influx for each grain size at the upper tainter gates. These values (Table 2) were determined by taking the amount of sediment that was leaving the model at the downstream end and appying it as an incoming load at the upstream boundary. The model needed some incoming supply of sediment to allow it to approach equilibrium and not be sediment starved and continuously scour away the bed. Multiple starting bed characteristics were tested to determine which combination best represented the existing conditions post initialization. Areas that were determined to not erode were assigned a bed layer thickness of zero. This included the stone weir, fossil beds, non-erodible vegetation, and upstream boundary material types (Figure 6). In the other areas where erosion could occur, a coarser material was placed on the bottom of the bed with a finer gradation specified as the top layer. This top layer allowed the river easy access to finer sediments and the ability to redistribute them to more realistic locations. Starting bed characteristics for each material type pre-intiailization that resulted in the best match are in Table 3. The four corresponding bed gradations from the table that were used in the model are plotted in Figure 9.

Figure 8. Bed sample locations.

Table 1. Grain sizes.

Classification	Grain Diameter (mm)
Very Fine Sand (VFS)	.088
Fine Sand (FS)	.177
Medium Sand (MS)	.353
Coarse Sand (CS)	.707
Very Coarse Sand (VCS)	1.41
Very Fine Gravel (VFG)	2.82
Fine Gravel (FG)	5.65
Medium Gravel (MG)	11.3
Coarse Gravel (CG)	22.6
Very Coarse Gravel (VCG)	45.2

Table 2. Influx sediment boundary condition.

Grain Classification	VFS	FS	MS	CS	VCS	VFG	FG	MG	CG	VCG
Influx (kg/s)*	40	10	10	10	10	10	10	1	0	0

*kilograms per second

Table 3. Starting bed characteristics pre-initialization.

Material Type	Top Gradation ID#	Top Thickness (meter)	Bottom Gradation ID#	Bottom Thickness (meter)
Navigation Channel	608R	0.3	611 L	5
Erodible Large Vegetation	606.7 Chute	0.1	606 L	0.4
Erodible Small Vegetation	606.7 Chute	0.1	606 L	0.4
Fossil Bed	NA	0	NA	0
Non Erodible Small Vegetation	NA	0	NA	0
Non Erodible Large vegetation	NA	0	NA	0
Stone Weir	NA	0	NA	0
Upstream Boundary	NA	0	NA	0
Focus Area	606.7 Chute	0.1	606 L	0.4

Figure 9. Starting bed gradation curves.

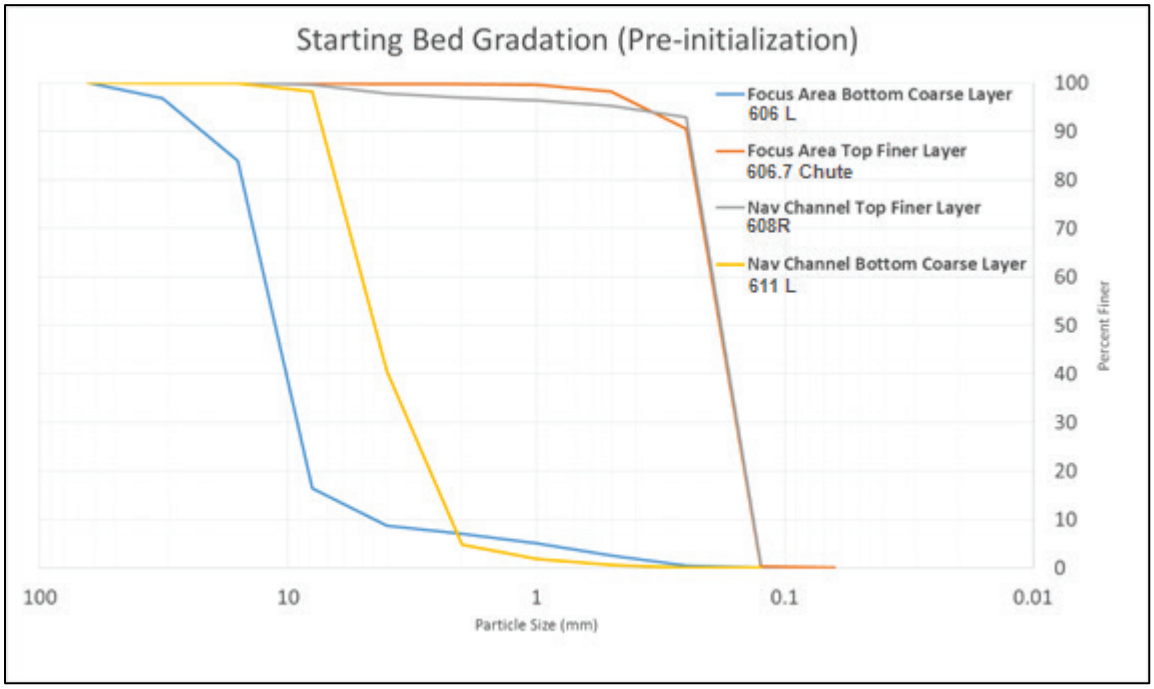

3 Model Calibration

The model was calibrated using field data collected by the CHL Field Data Collection Branch during July 2016. Collected data used for calibration included water surface elevations, velocity profiles, and bed gradation samples.

3.1 Hydraulic calibration

The model was used to simulate the gate releases and tailwater conditions on the day of the field data collection, 8 July 2016. These controlled boundary conditions for that day are listed in Table 4. Roughness values were assigned and adjusted to match the measured water surface and velocity profiles. Final calibrated Manning's *n* values are shown in Table 5.

Table 4. Hydraulic calibration boundary conditions.

Upstream Gate Discharge (cfs)*	53,364
Downstream Gate Discharge (cfs)	13,914
Powerhouse Discharge (cfs)	28,004
Downstream water surface elevation (ft)	389.04

*cubic feet per second

Table 5. Roughness values.

Material Type	Manning's *n*
Navigation Channel	0.0235
Erodible Large Vegetation	0.05
Erodible Small Vegetation	0.035
Fossil Bed	0.025
Non Erodible Small Vegetation	0.035
Non Erodible Large Vegetation	0.05
Stone Weir	0.04
Upstream Boundary	0.025
Focus Area	0.0235

The field data team provided three measured water surface profiles (Figure 10). Modeled water surface elevations in the same location as the measured field data are plotted together for all three locations. The results

of these comparisons for the final calibrated roughness values are shown in Figures 11 through 13. Water surface profiles are plotted with upstream on the right and downstream on the left to match the orientation of the locations in Figure 10.

Figure 10. Location of water surface profiles.

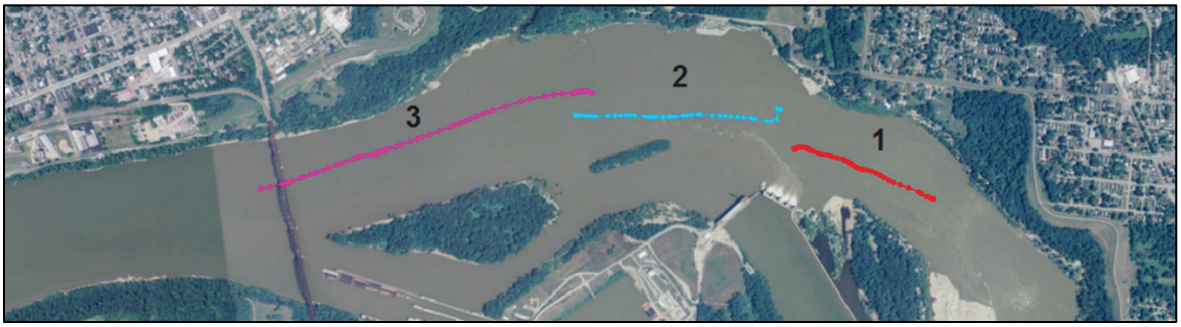

Figure 11. Water surface Profile 1 comparison.

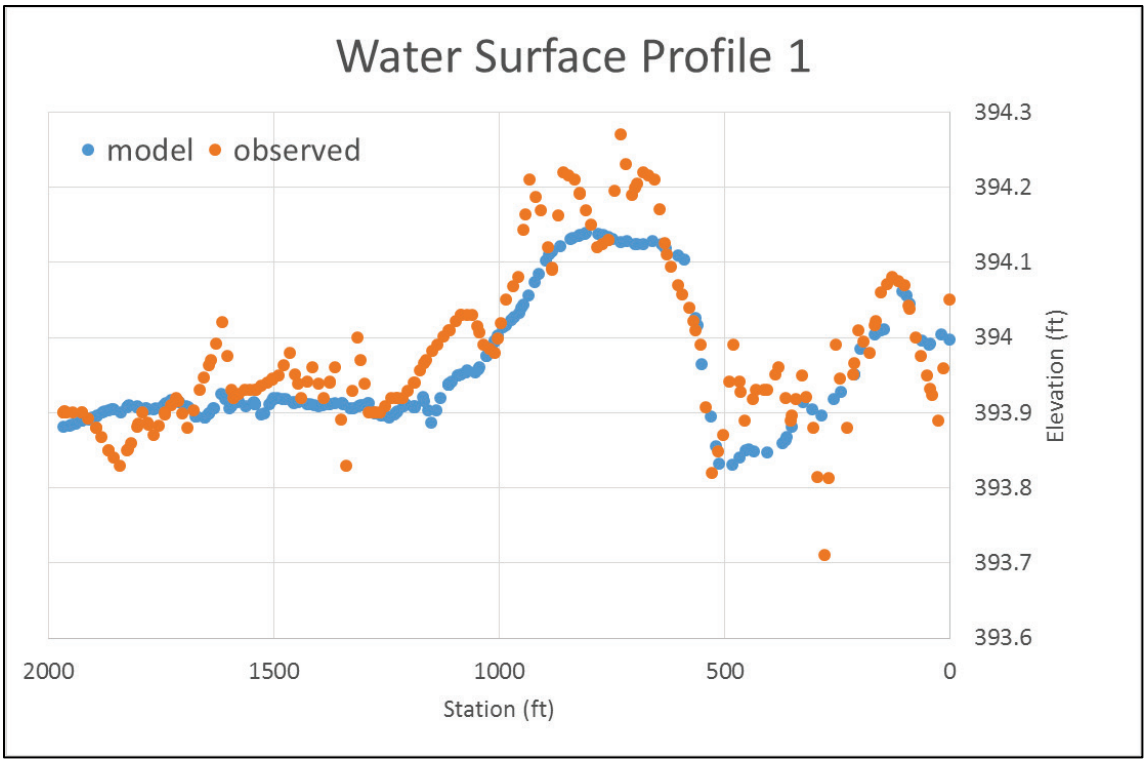

Figure 12. Water surface Profile 2 comparison.

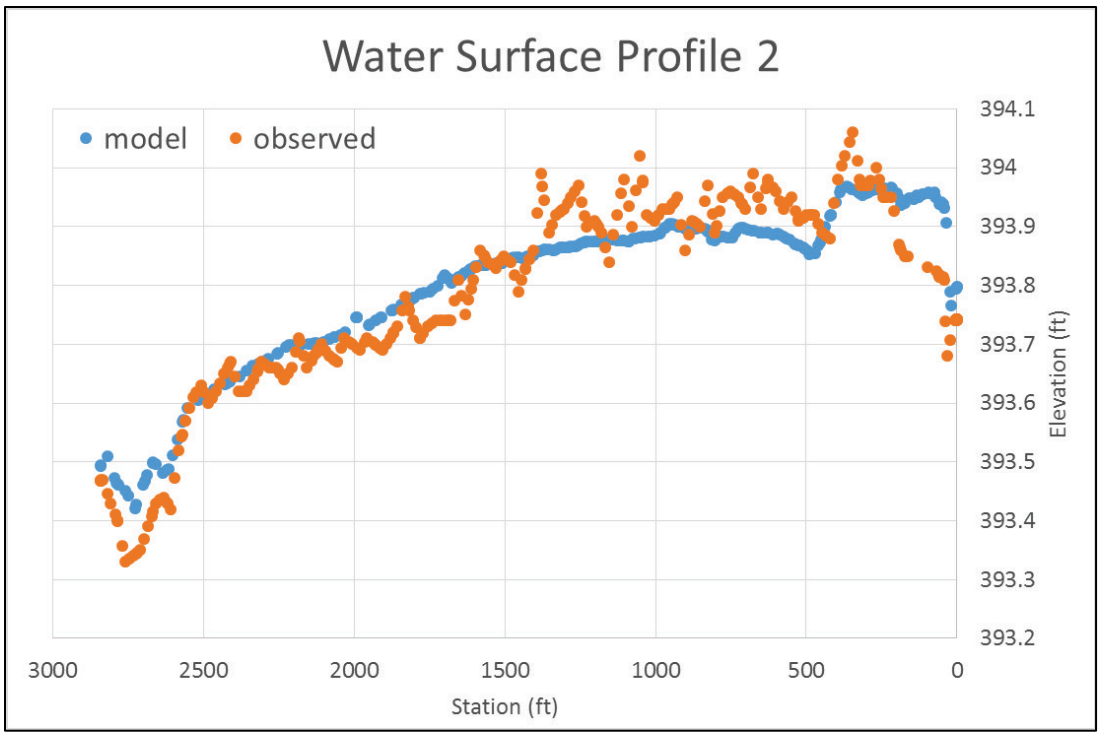

Figure 13. Water surface Profile 3 comparison.

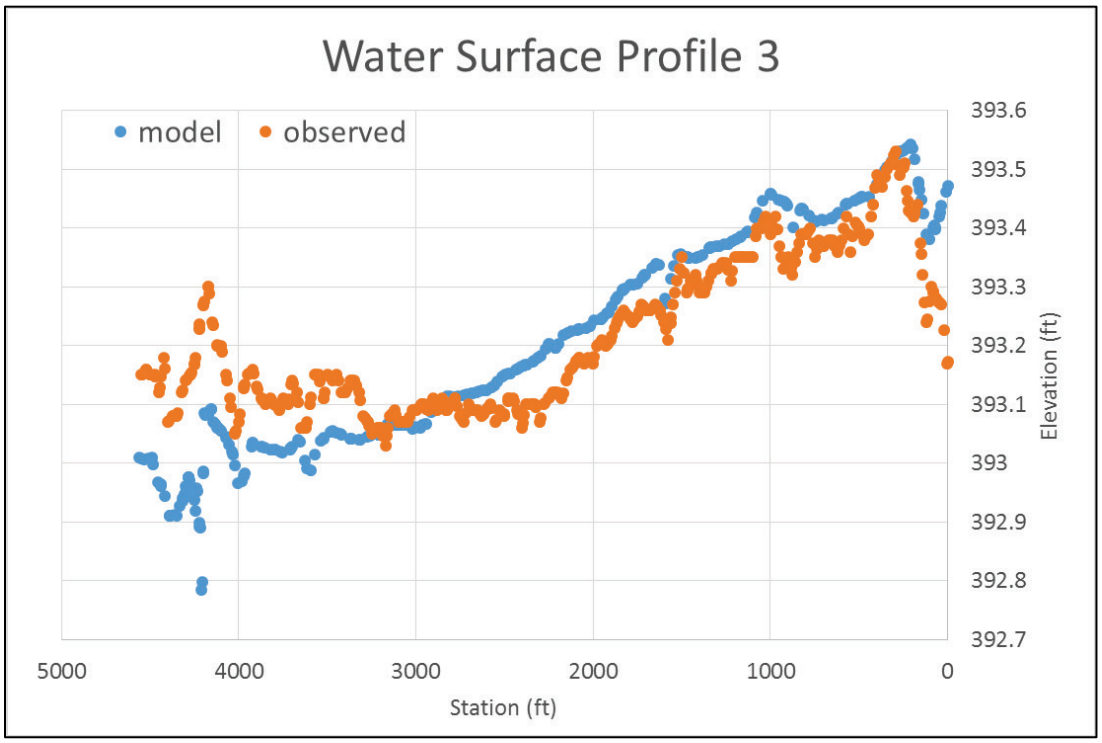

Most of the modeled water surfaces are within the scatter of the measured data or within one-tenth of a foot. The model and the measured data diverge some at the downstream end of Profile 3. The modeled water surfaces are still within 0.2 to 0.3 ft of the measured data at this location. This divergence is likely due to the close proximity of the data to a bridge pier. There is some roughness added by the bridge piers and possible vertical velocities that cause the increase in water surface observed in the measured data. The bridge piers are clipped out of the model resulting in a constriction of the area of flow, so this observed increase is not completely captured by the model. The model is able to capture the drawdown that occurs over the submerged weir at the upstream end of Profile 3 and the downstream end of Profile 2. The model is also able to reproduce the drawdown and rise of the water surface seen in Profile 1.

Model results were also compared to depth-averaged velocities measured by the field data team. Figure 14 maps the location of these four measured velocity profiles. Model and measured velocities for each profile are compared in Figure 15 through Figure 18. Stationing is oriented from left descending bank to right descending bank.

Figure 14. Velocity profile locations.

Figure 15. Velocity Profile 1 comparison.

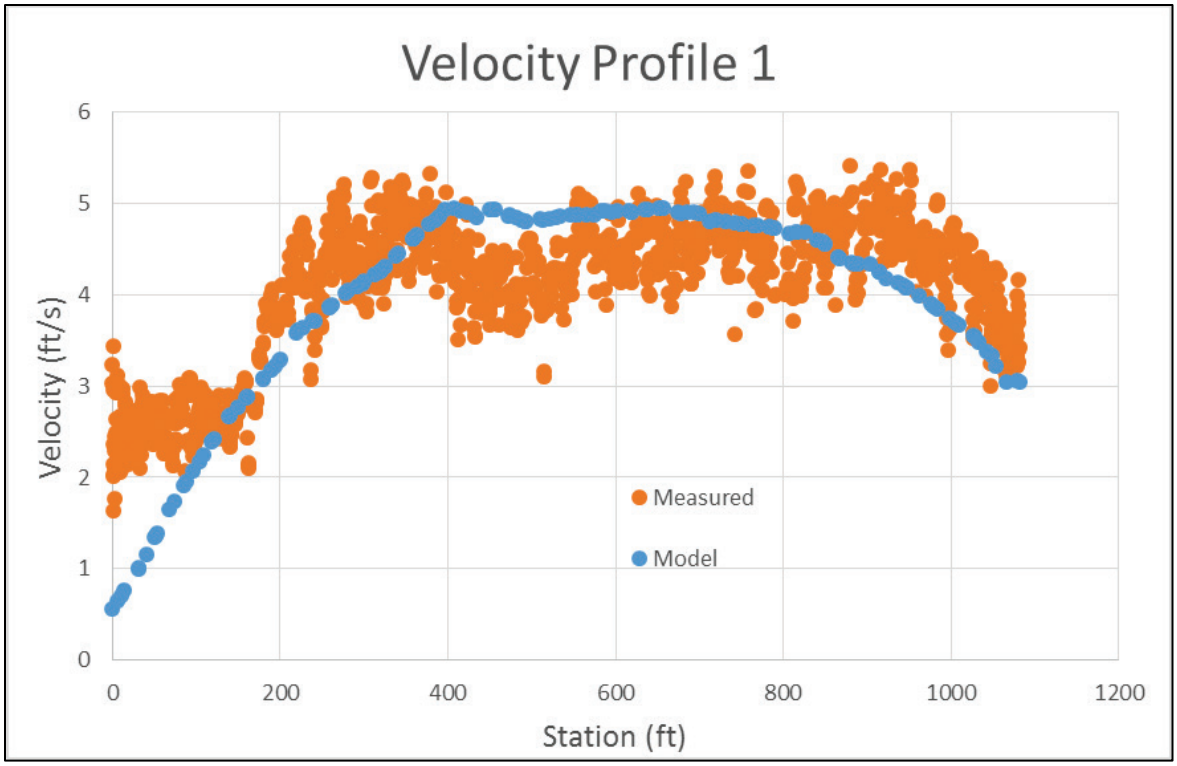

Figure 16. Velocity Profile 2 comparison.

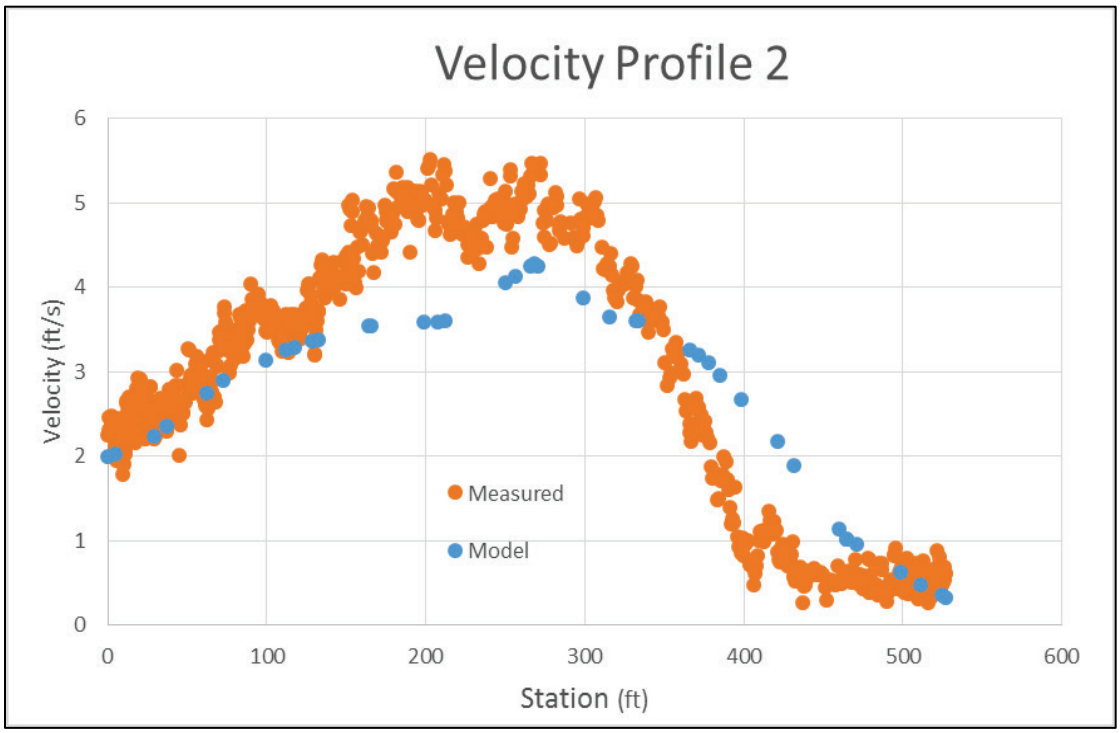

Figure 17. Velocity Profile 3 comparison.

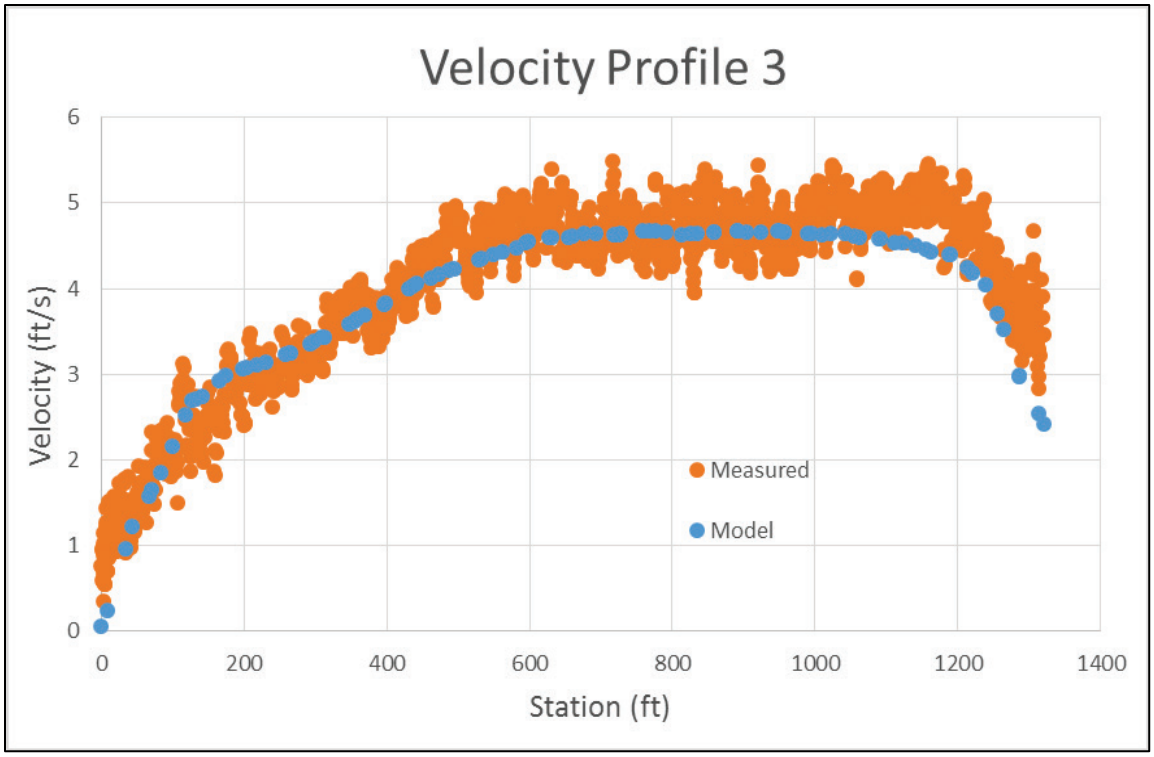

Figure 18. Velocity Profile 4 comparison.

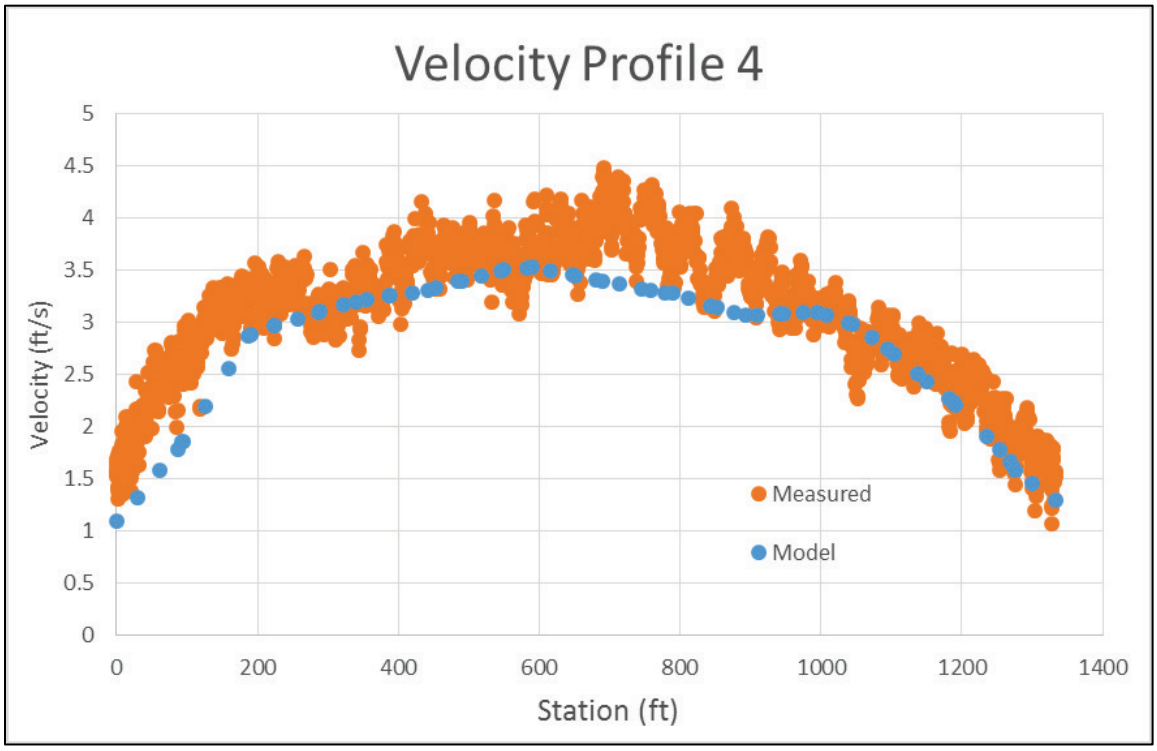

Overall, modeled velocity profiles match the measured data accurately. Profiles 1 and 3 were given priority as they were the closest proximity to the bank where the erosion has occurred in the past. Profiles 2 and 4 do not match as well as 1 and 3, but they still are well representative of the actual conditions. These velocity profiles ensure that the flow split around the large island is accurately captured by the model.

3.2 Sediment calibration

Sediment calibration was performed by comparing post initialization bed gradations and thicknesses to the measured data once the 100-day initialization run was completed (discussed in Section 2.3). The sediment data were extracted from the model and compared to the measured field data in the area of interest both quantitatively and qualitatively. Modeled gradations were compared to the measured bed sample gradations while bed thicknesses were compared using bed sample sizes and images of the site. The samples' locations that were used for comparison are mapped in Figure 19. The blue locations are where adequate-sized field samples were obtained and are compared to the resulting modeled gradations (Figure 20).

Figure 19. Location of bed samples used for comparison.

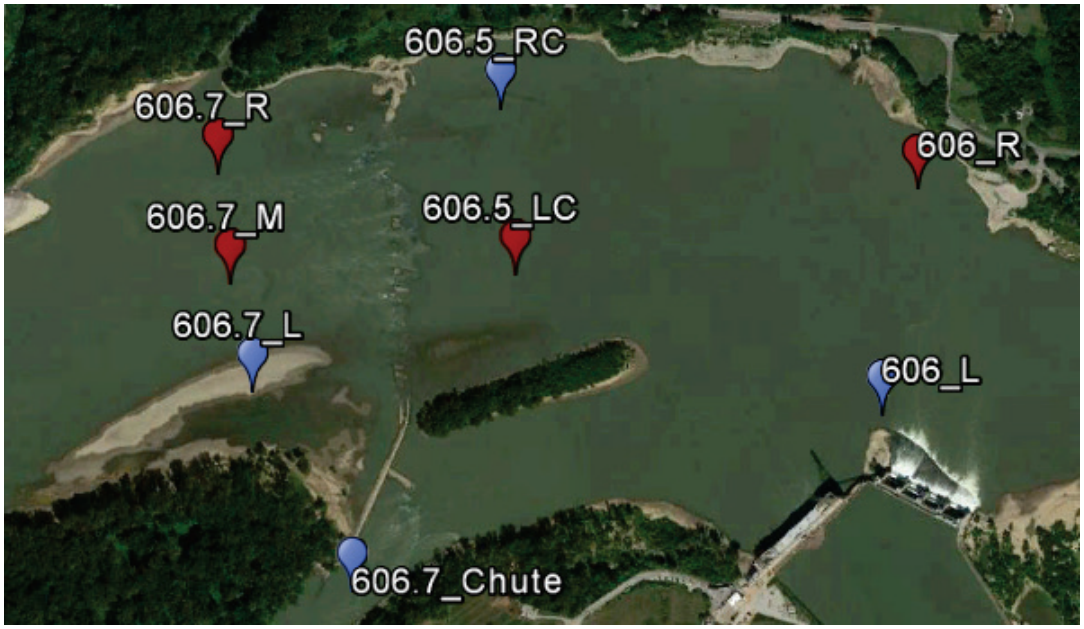

Figure 20. Modeled and measured gradation comparison.

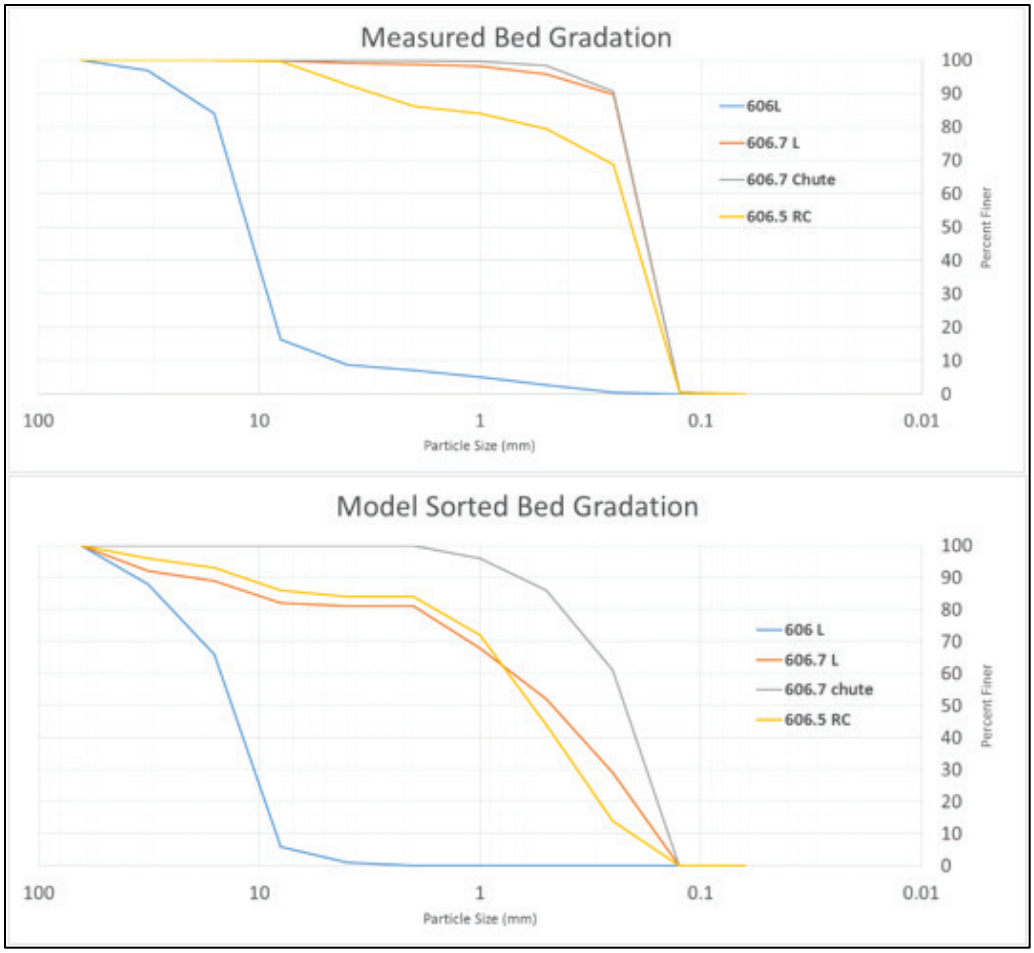

Model gradations were taken from only the active layer in the model. This is the layer of sediment that includes the top-most portion of the bed, which is representative of what would be collected by a physical sediment-scooping sample device. The curves in Figure 20 depict the model's ability to replicate observed gradation trends in the field.

The red sample locations in Figure 19 are samples that did not have a substantial amount of sediment reported. In discussions with the field data collection team, it was determined that hard surfaces such as bed rock or limestone existed in these locations. Multiple attempts were made to collect samples in these locations, but were unsuccessful, often feeling the sampler scraping across the hard bottom surface. The presences of a hard surface in these areas is consistent with what is exposed above the water surface during low-flow conditions downstream of the upper tainter gates. This information was used to compare bed layer thickness values in the model.

Areas where non-erodible material or hard points are located can be replicated by the model if the model scours the sediment off the bed during the initialization resulting in a bed layer thickness near zero. Figure 21 shows total bed layer thickness and a map of locations (zones) that can be compared with aerial images where exposed rock or deposition is observed. Red contours or areas of no color within the model limits represent areas where the higher velocities have flushed out the sediment resulting in a hard point in the model. These areas match up well with what can be seen in zones 1 and 2 in the figure and the location of the red samples in Figure 19. Conversely, the blue contours represent areas where deposition has occurred resulting in a larger bed thickness. Zones 3, 4, and 5 are examples of where the model was able to replicate depositional sites that can be seen in the aerial imagery. Figure 22 through Figure 26 depict enlarged views of zones 1–5 in Figure 21. Zones 1 and 2 (Figures 22 and 23) are in areas of high energy where a high transport capacity does not allow sediment deposition to occur. This can be observed in the figures as hard points such as areas where bedrock or large stones are exposed with no sediment deposited on top of them. Sand and finer sediment deposits can be seen in Zones 3, 4, and 5 in Figures 24–26. These are areas of lower energy with less transport capacity where sediment is able to deposit.

Overall the model was able to satisfactorily replicate measured field conditions. The hydraulic and sediment calibration provides confidence that the model can be used to accurately simulate and compare different scenarios.

Figure 21. Model bed layer thickness and close-up comparison locations.

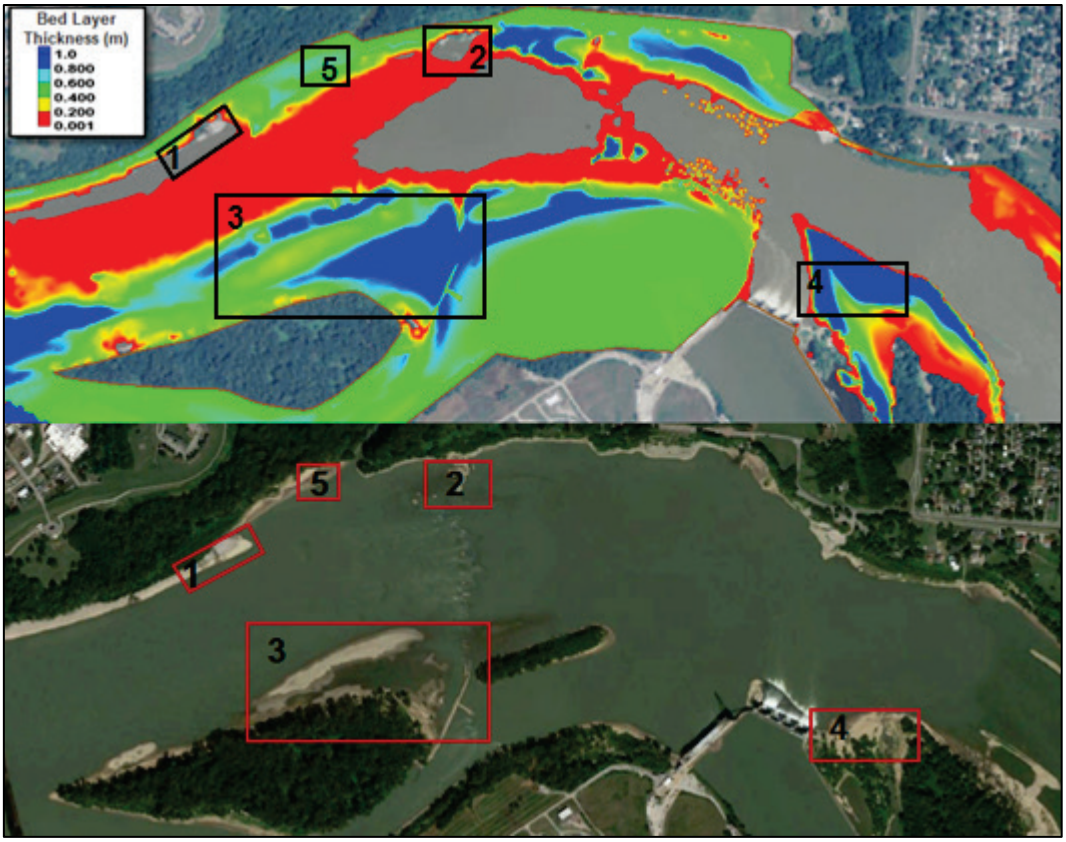

Figure 22. Zone 1.

Figure 23. Zone 2.

Figure 24. Zone 3.

Figure 25. Zone 4.

Figure 26. Zone 5.

4 Existing Causes

To determine a *worst-case* scenario, gate operations were simulated to determine which combination impinges on the eroding bank the most. Due to uncertainty of an exact operating schedule, a relatively high flow and low flow were modeled with varying flow distributions between the upper and the lower gates. The chosen day of the low flow was 1 July 2007. This date was chosen because there is an aerial image from that day when all the flow was through the lower gates, which appears to be one of the worst-case scenarios because currents and wakes can be seen heading directly to the opposite bank (Figure 27). The total flow on this date was 24,900 cfs. The 28 February 2016 flow was also chosen due to there being high flow, which was also captured by aerial imagery (Figure 34). The flow on this date was 328,000 cfs. To cover a range of operations, total flow in the model for both the high and low flow was held constant while the distribution between the upper and lower gates was varied. Modeled velocity magnitude and direction results for the low-flow condition with the varying distributions in 20% increments are shown in Figures 28–33. High flows are depicted in Figures 35–40. Velocity patterns are the only results plotted as they were determined to be a better comparison of the conditions at the bank than bed displacement. Velocity patterns were more informative as the specific erosion problem was outside of typical 2D sediment model uses. The 2D sediment model is not capable of simulating local scour and vertical bank failure and is more often used for determining general shoaling and erosional areas within main channels. The sediment calibration still provides validation of the hydraulics as accurate hydraulics are needed to replicate sediment trends.

Figure 27. Low-flow aerial image.

Figure 28. Low-flow 0-100 split velocities.

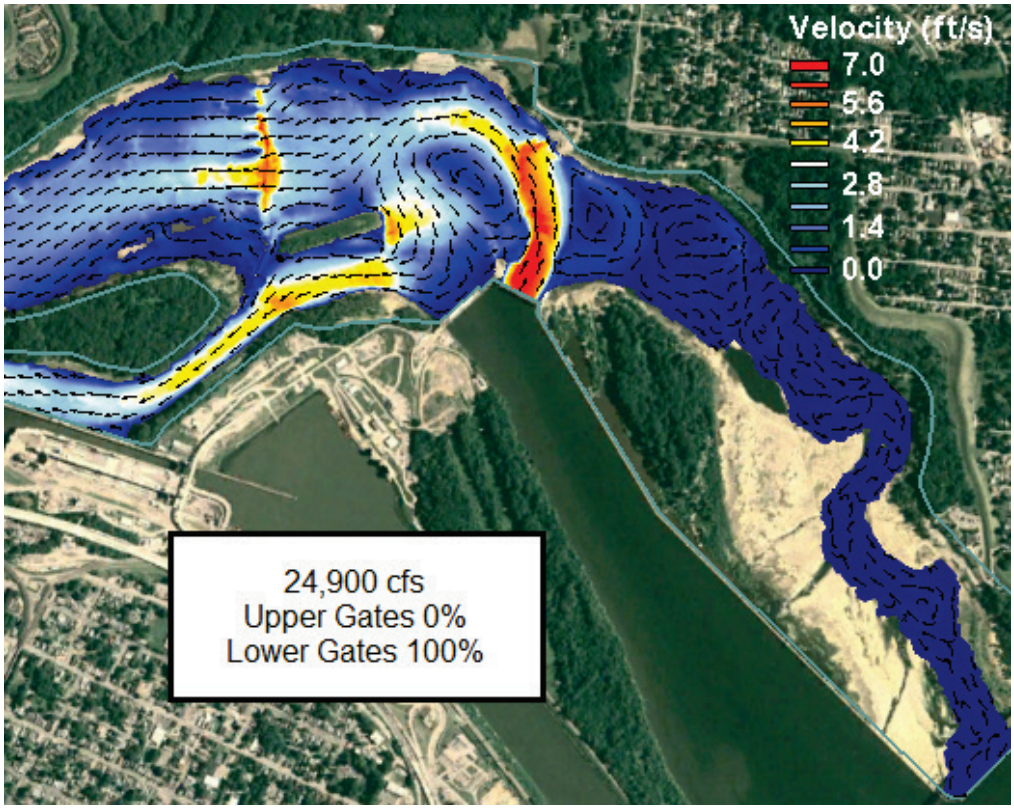

Figure 29. Low-flow 20-80 split velocities.

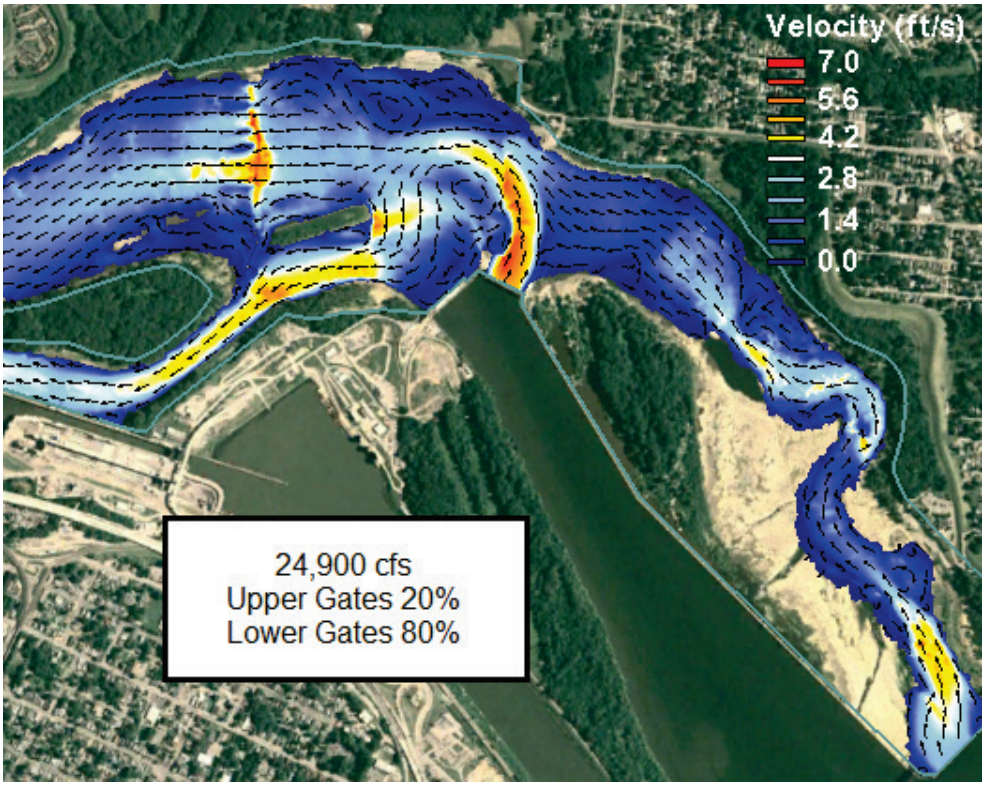

Figure 30. Low-flow 40-60 split velocities.

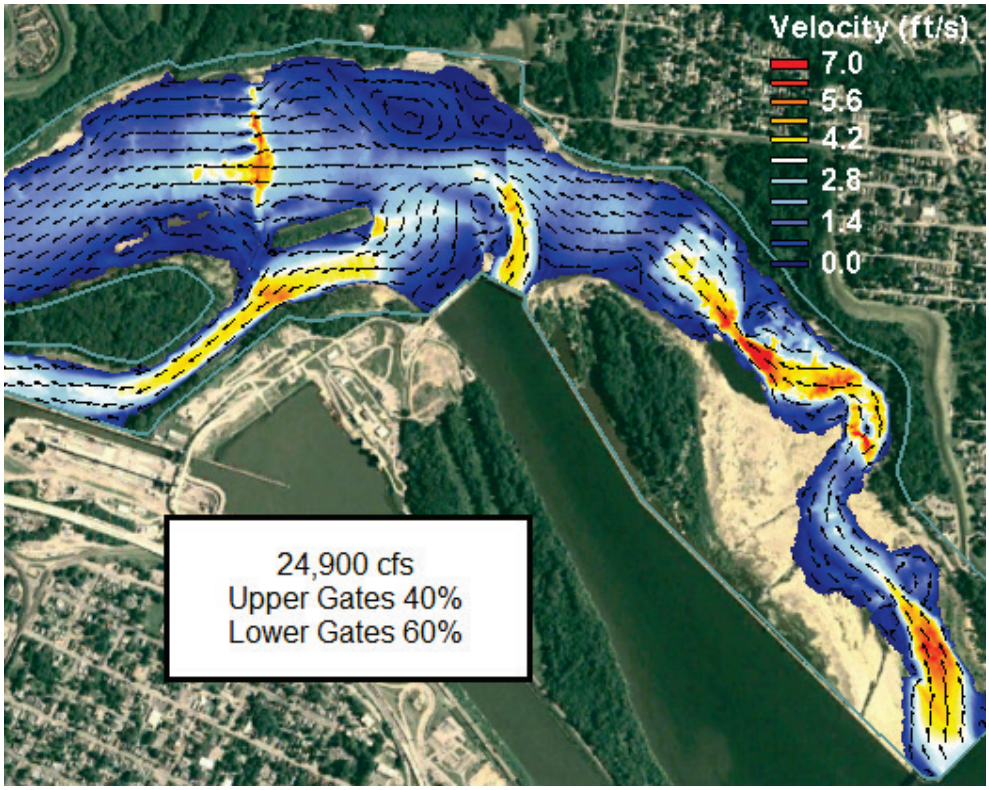

Figure 31. Low-flow 60-40 split velocities.

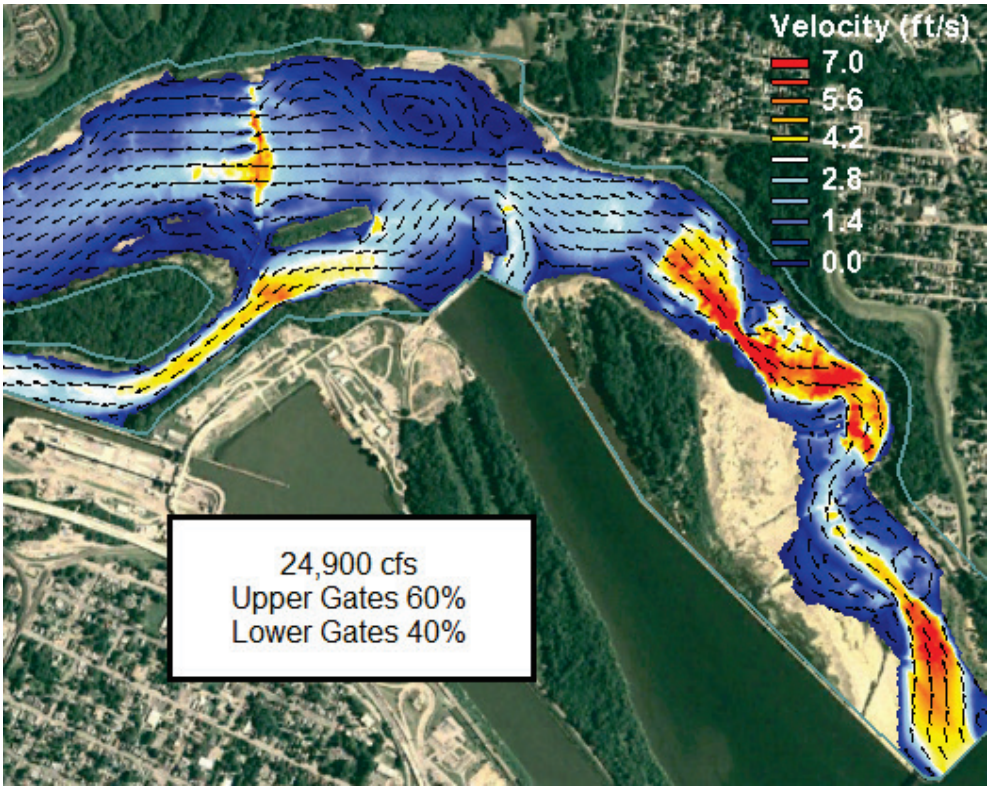

Figure 32. Low-flow 80-20 split velocities.

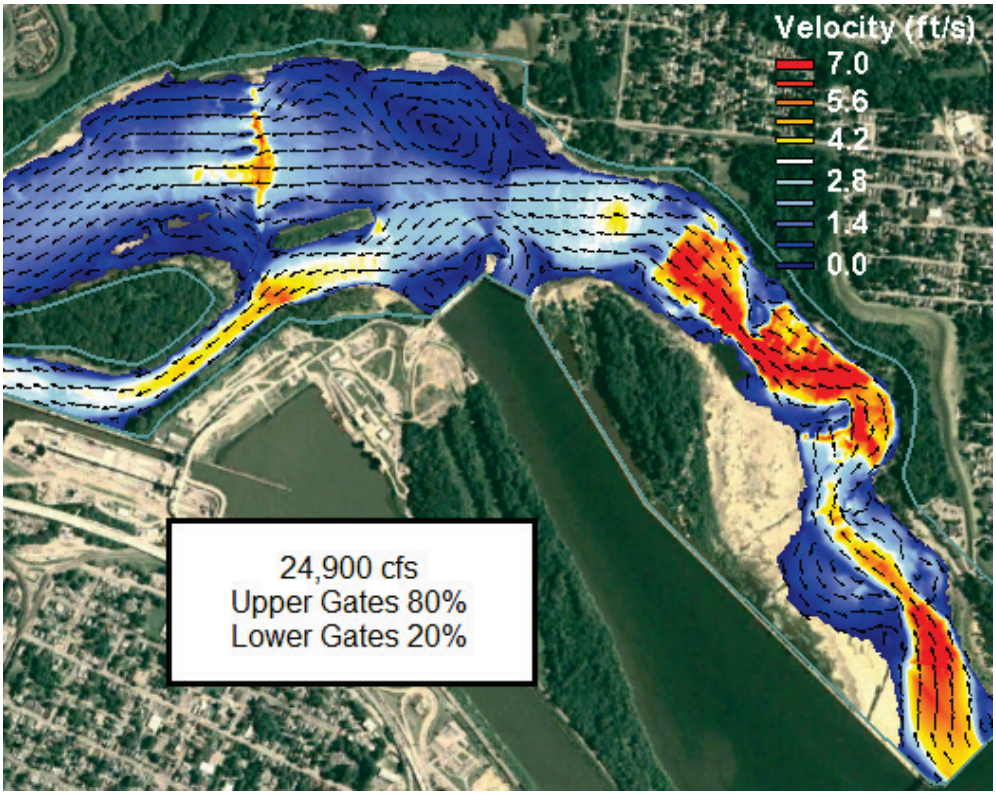

Figure 33. Low-flow 100-0 split velocities.

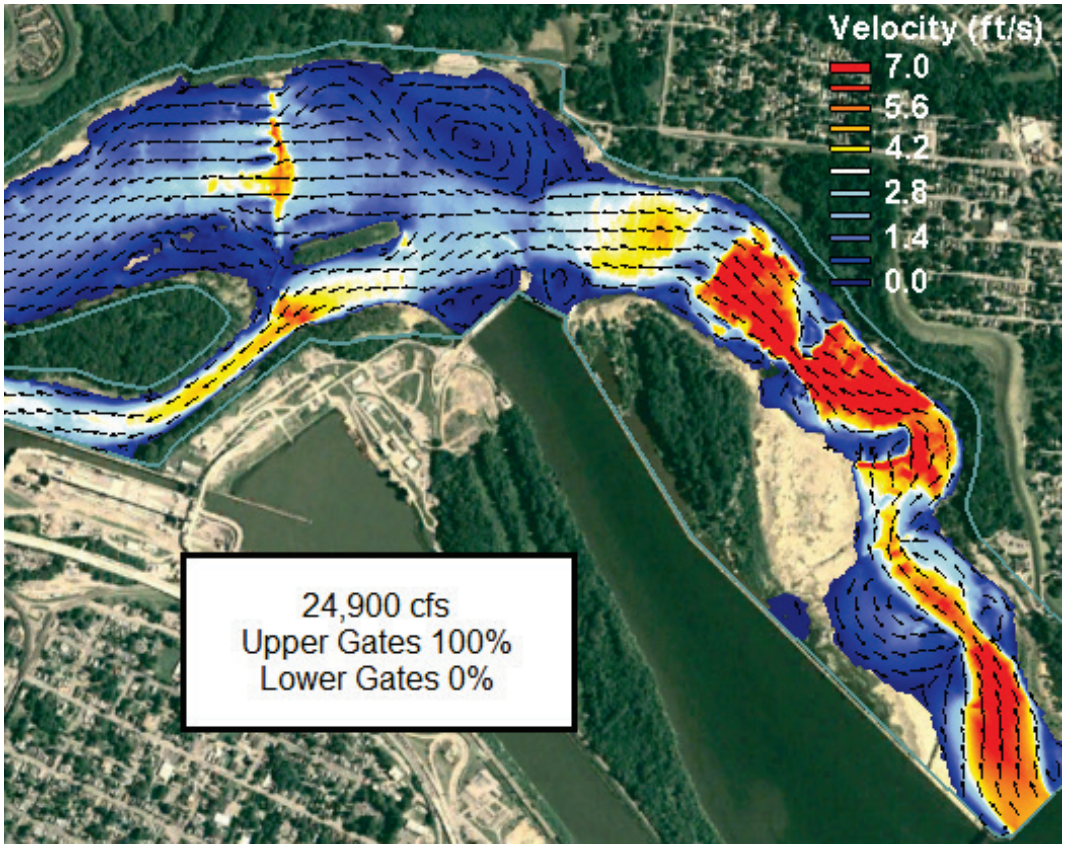

Figure 34. High-flow aerial image.

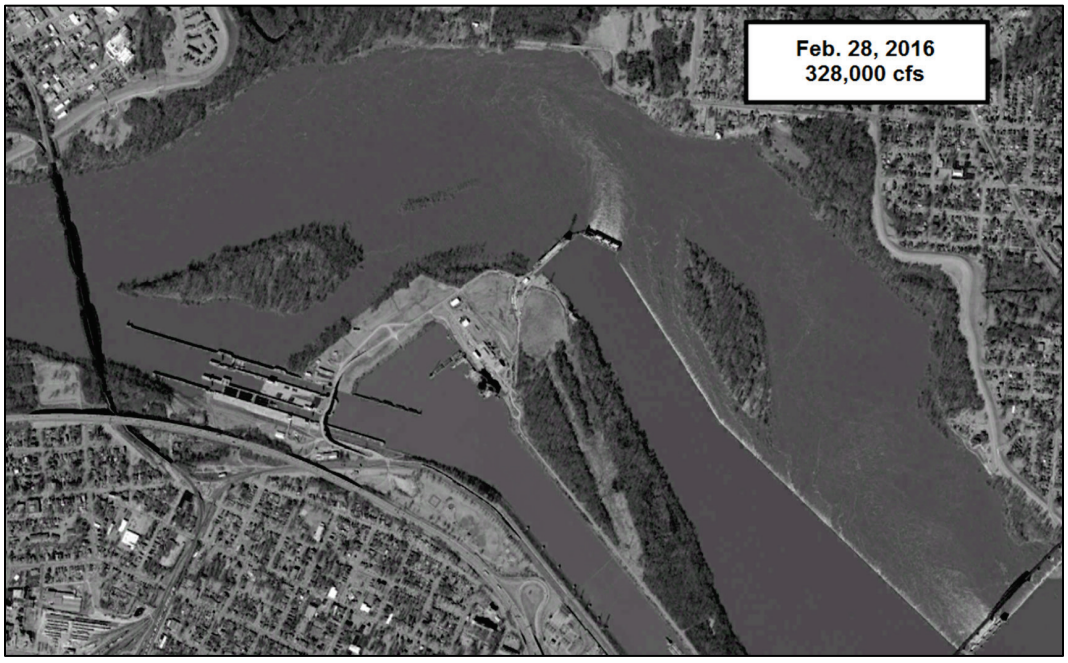

Figure 35. High-flow 0-100 split velocities.

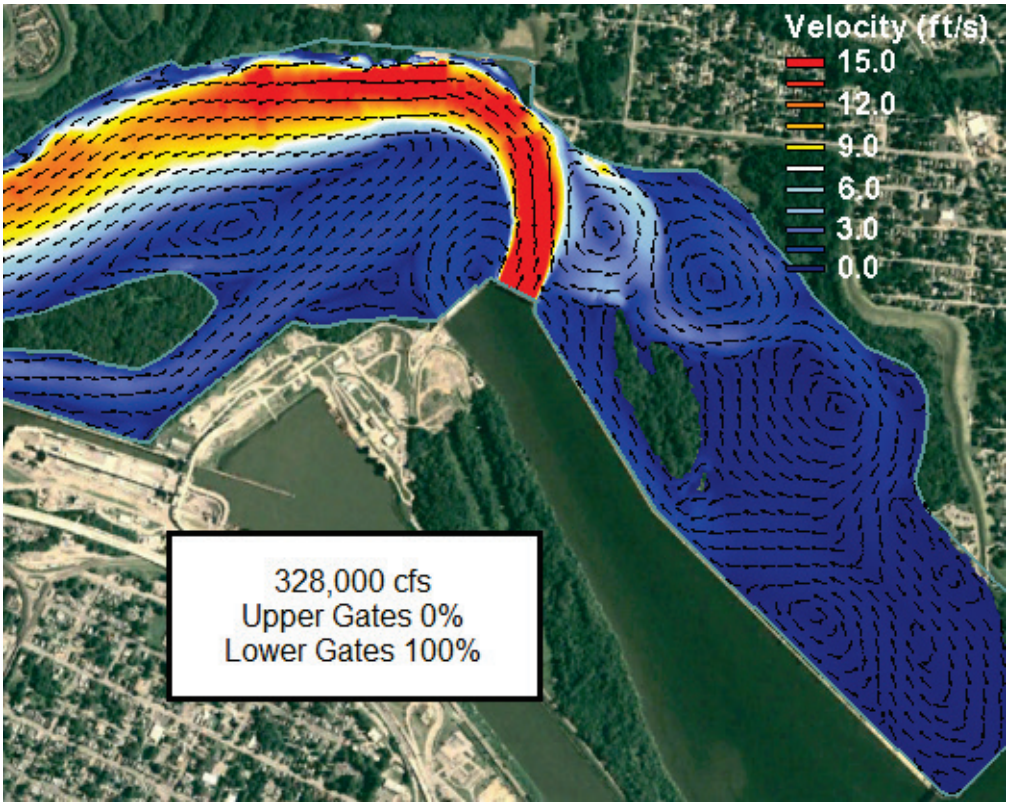

Figure 36. High-flow 20-80 split velocities.

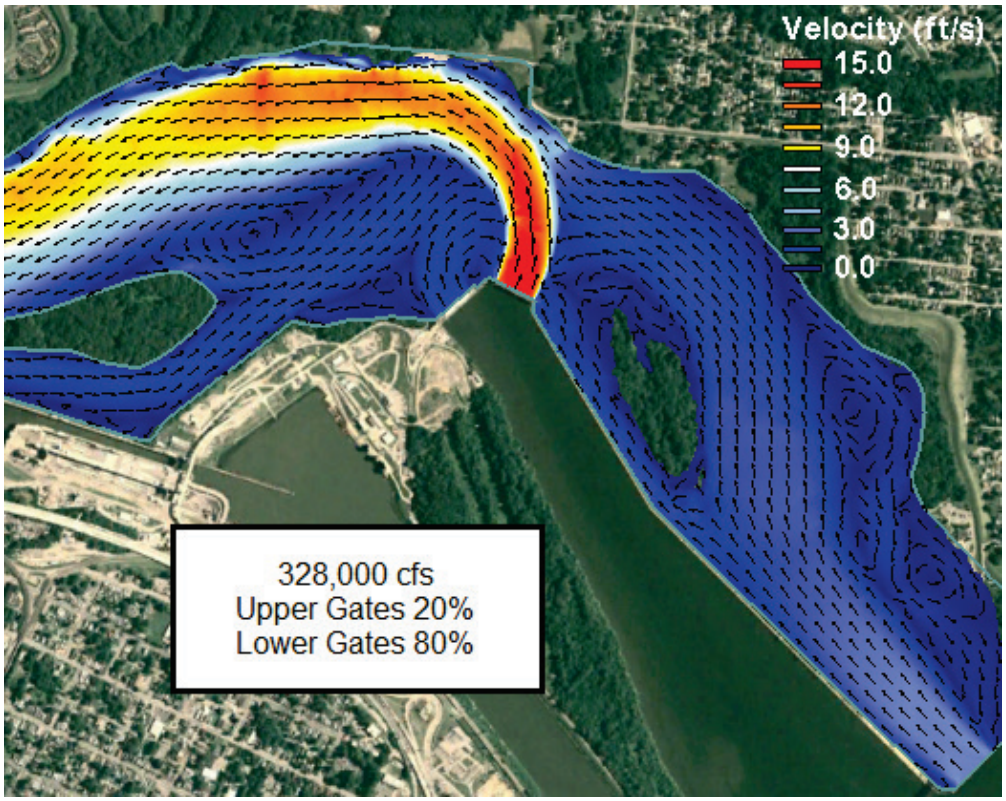

Figure 37. High-flow 40-60 split velocities.

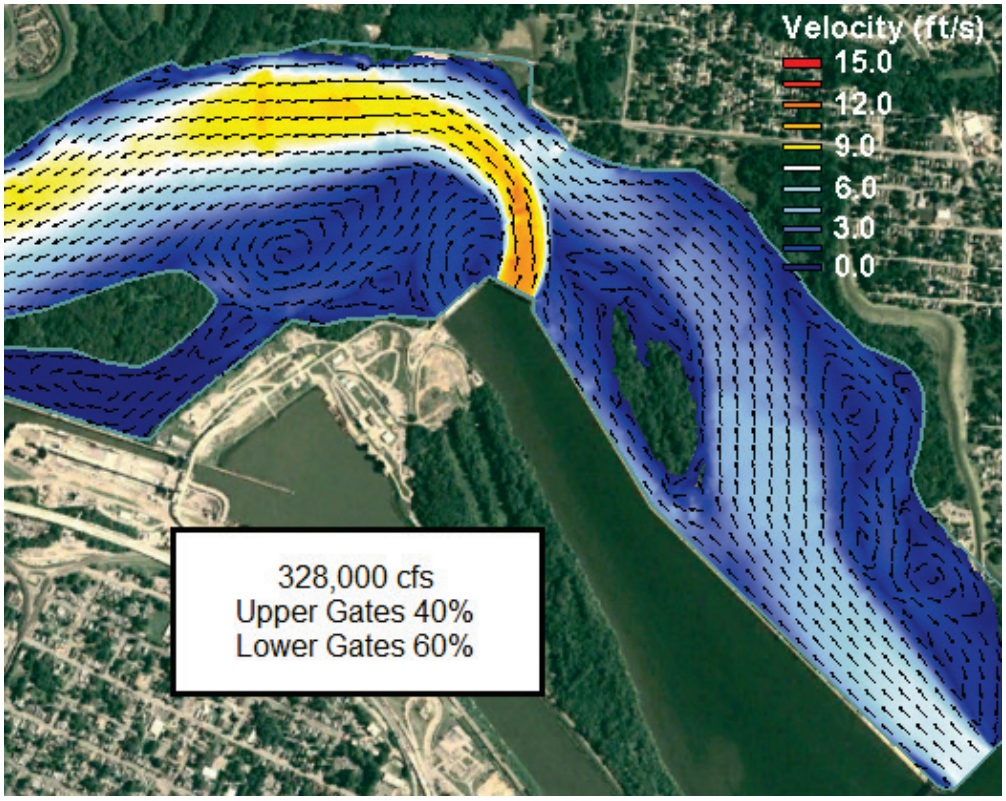

Figure 38. High-flow 60-40 split velocities.

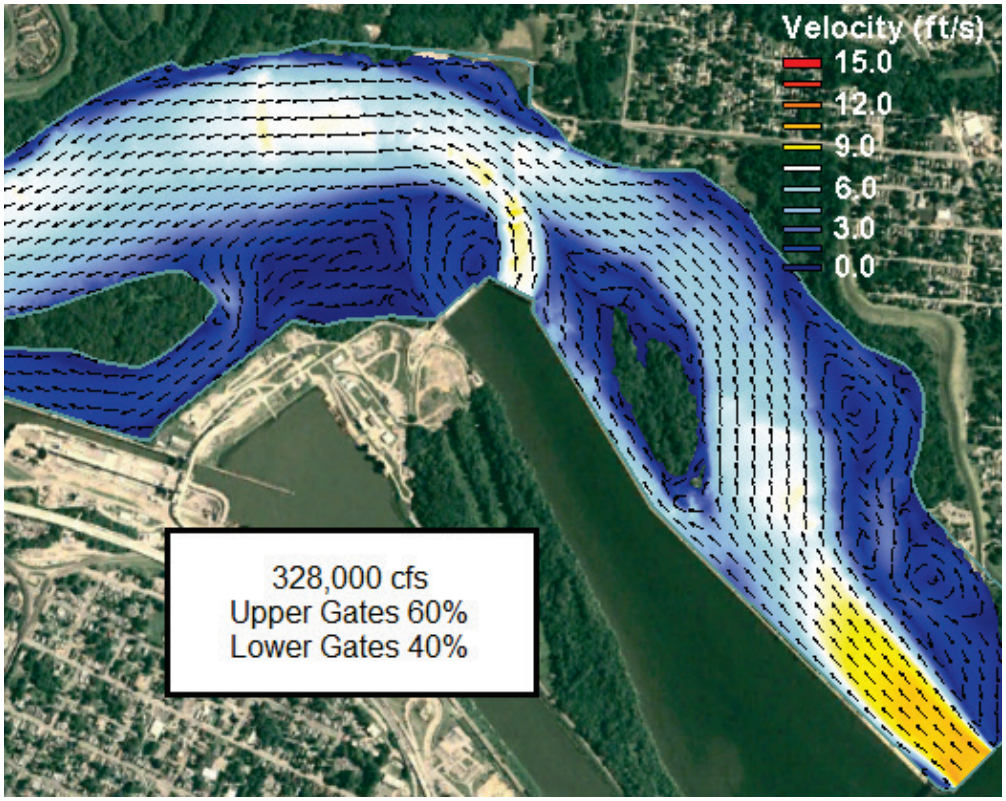

Figure 39. High-flow 80-20 split velocities.

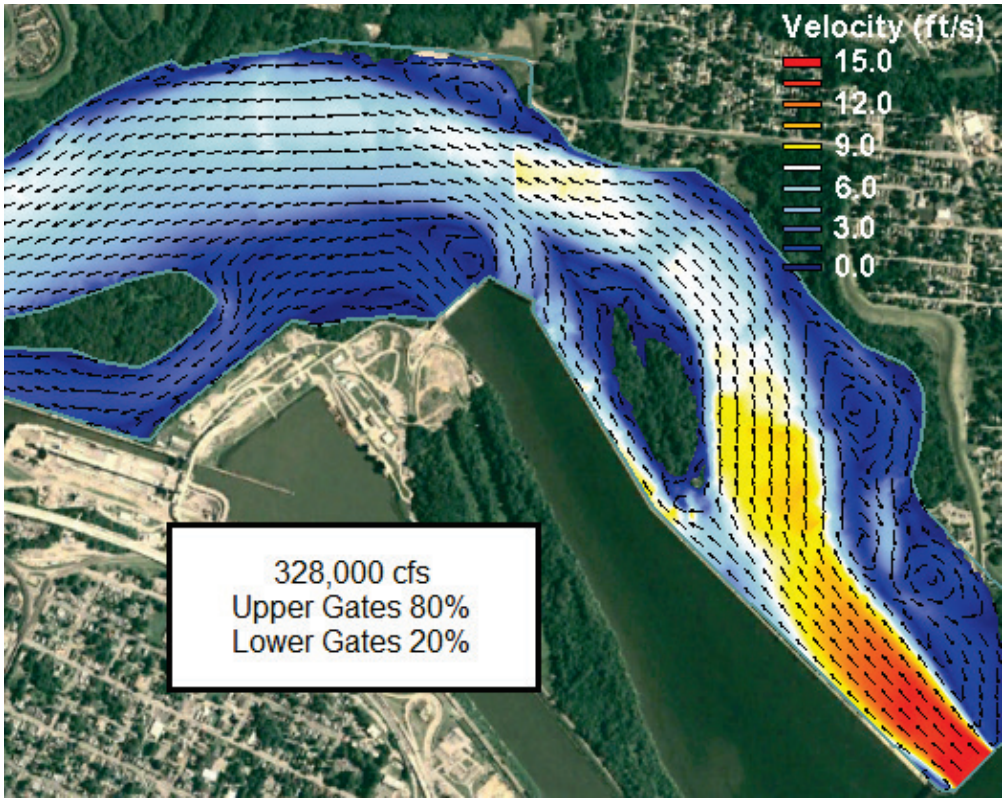

Figure 40. High-flow 100-0 split velocities.

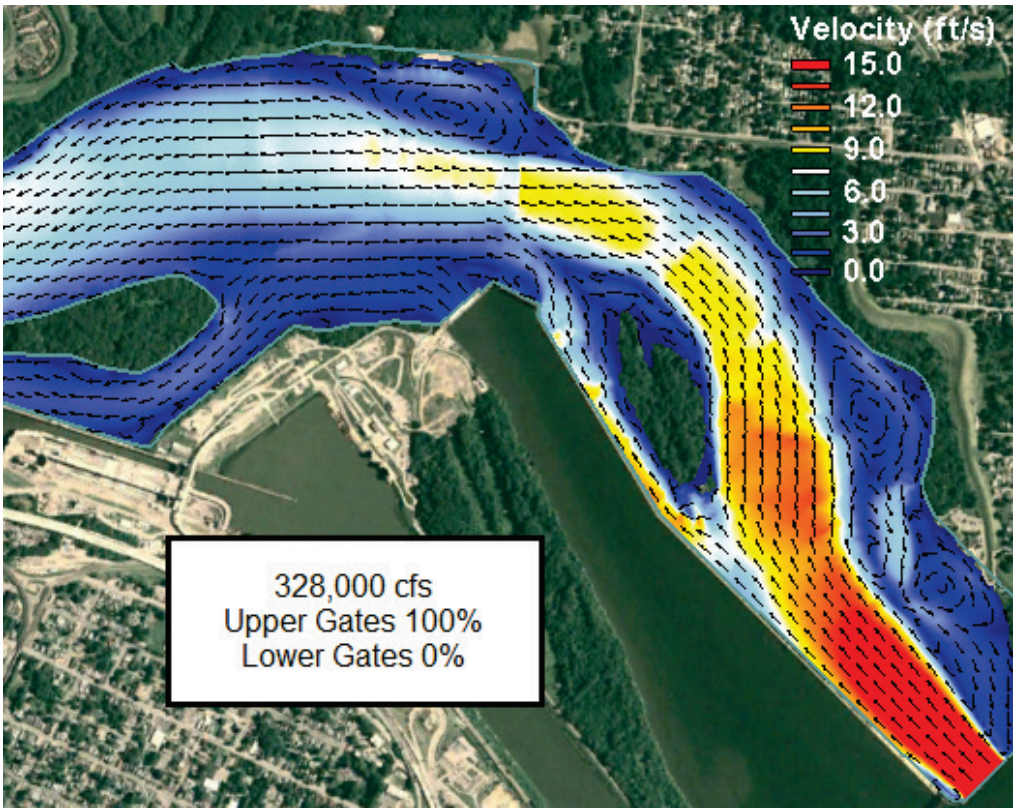

For both the low- and high-flow conditions, the highest velocities in the problem area occur when 100% of the flow is passing through the lower gates. However, at the higher flow of 328 thousand cubic feet per second (kcfs), passing all the flow through these gates is not possible. At this high flow rate, all gates are likely completely open passing as much flow as possible. This is evidenced by the flow that is overtopping the wall between the two sets of gates in Figure 34. A 40% upper-60% lower to 60% upper-40% lower range is likely the only physically possible gate distribution for this high of a flow, so they were the only percentage splits that were considered when determining the worst-case scenario for the model.

Figure 41–43 are a direct comparison of the velocities in the problem area for the worst-case low-flow and high-flow distributions. During the low-flow simulation, velocities do not reach 2 feet per second (fps) (shown in green in the image) until a substantial distance into the center of the channel. Velocities along the bank are all in the 0–1 fps range. The 60% upper-40% lower high flow split forms a large eddy with velocities in the 2–3 fps range along the bank. In the 40% upper-60% lower split, this eddy is reduced, but some higher velocities occur on the bank downstream of the eddy circulation. Depths for the low-flow and high-flow simulations are plotted in Figure 44 and Figure 45, respectively. The nearly 300,000 cfs difference in flow resulted in a 30 ft increase in the water surface elevation and a significant increase in the lateral extents of the water. This increase in depth results in more saturated soil on the bank and supports the idea that the problem is also a geotechnical issue. Geotechnical issues are outside the purpose of this hydraulic study and would require a separate analysis by geotechnical experts. The low-flow water levels are well below the bankline that has experienced erosion in the past. These results help to conclude that the high flow is a worst-case scenario for the bank.

Figure 41. 24,900 cfs 100% lower gates.

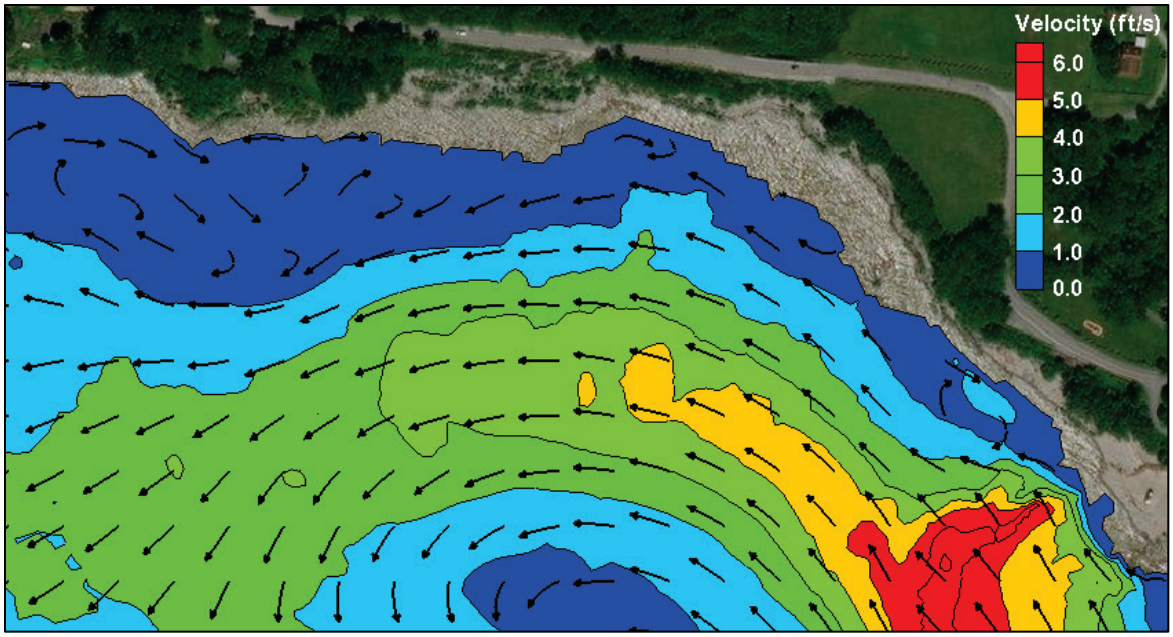

Figure 42. 328,000 cfs 60% upper 40% lower.

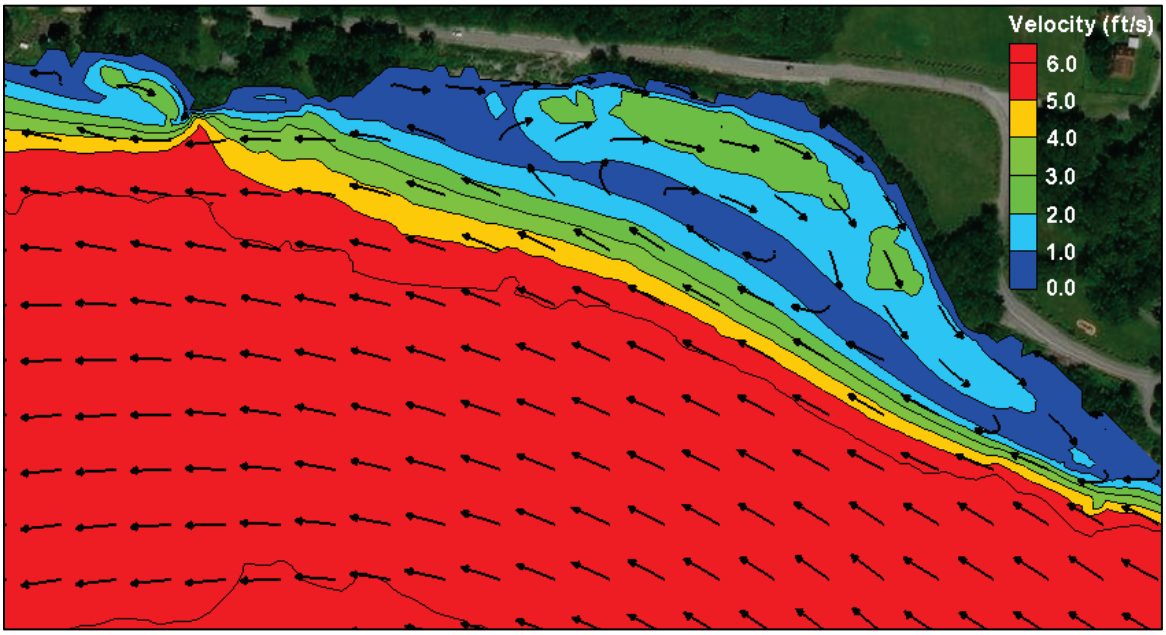

Figure 43. 328,000 cfs 40% upper 60% lower.

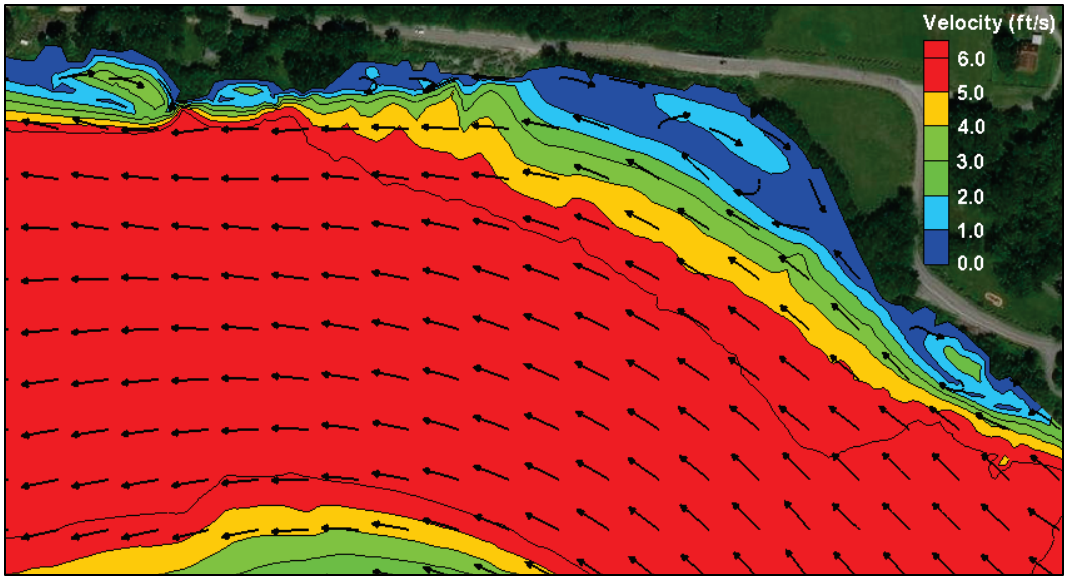

Figure 44. 24,900 cfs (low flow) depths.

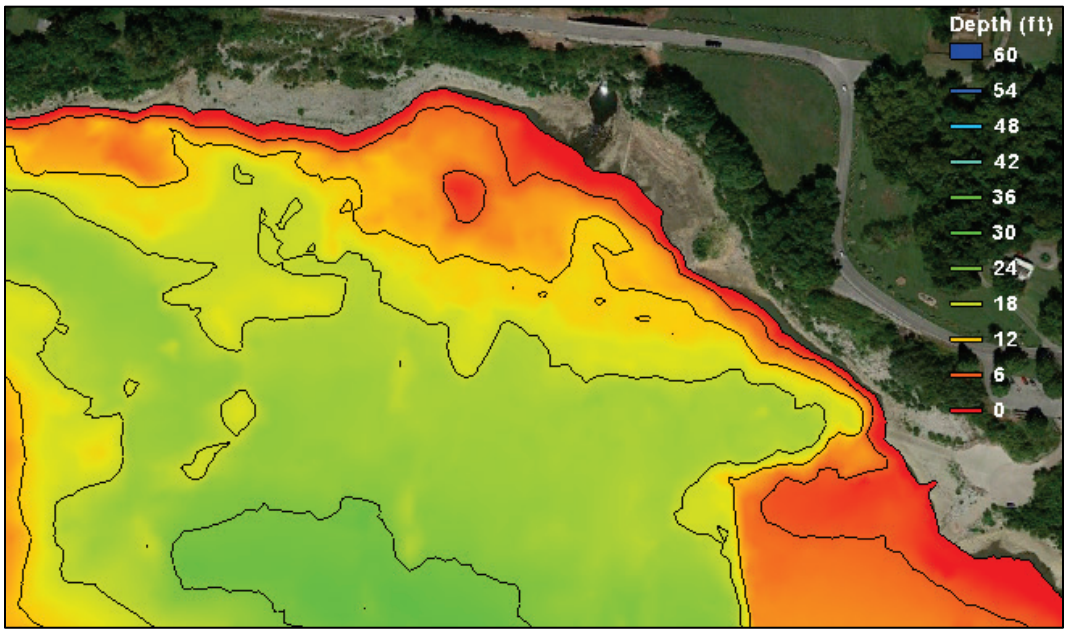

Figure 45. 328,000 cfs (high flow) depths.

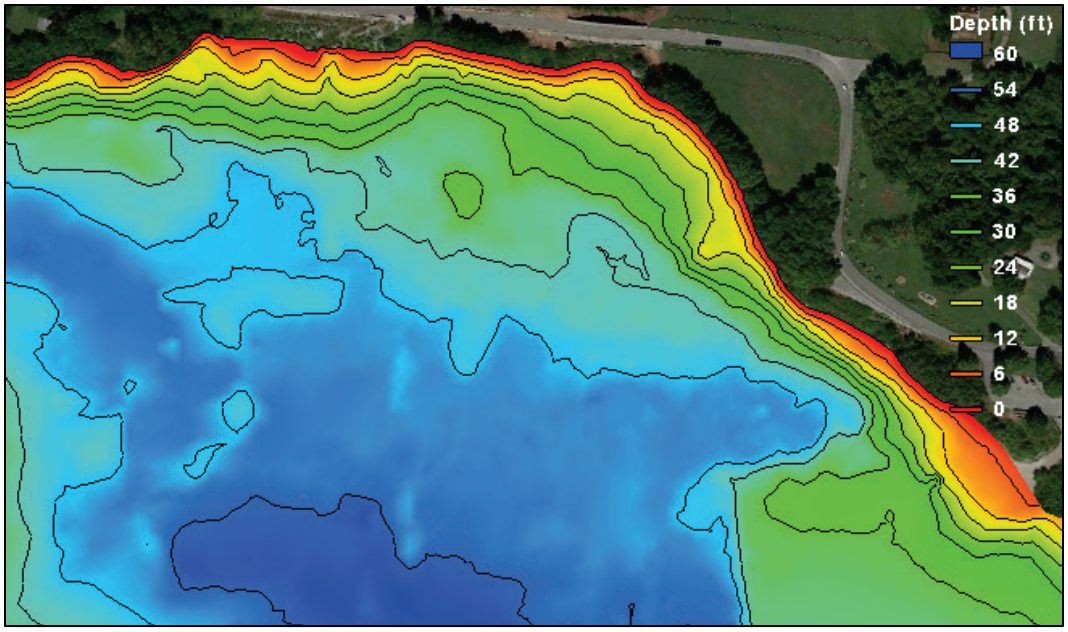

5 Proposed Alternatives

High-flow conditions for both the 60% upper-40% lower and 40% upper-60% lower split were simulated with five different structural alternatives or plans implemented in the model. Velocity patterns were the main result analyzed to determine the effectiveness of the plans. These plans include the following:

- Plan 1–Submerged bendway weirs
- Plan2–Emergent flow deflector and two small dikes
- Plan 3–System of small dikes
- Plan 4–Two dikes
- Plan 5–Four dikes.

Geometries for the five plans and the existing conditions are illustrated in Figure 46–51. Contoured elevations depict bathymetric and ground elevations of the different plans. Plans 2–5 are all emergent structures rising above the water surface.

Figure 46. Existing geometry.

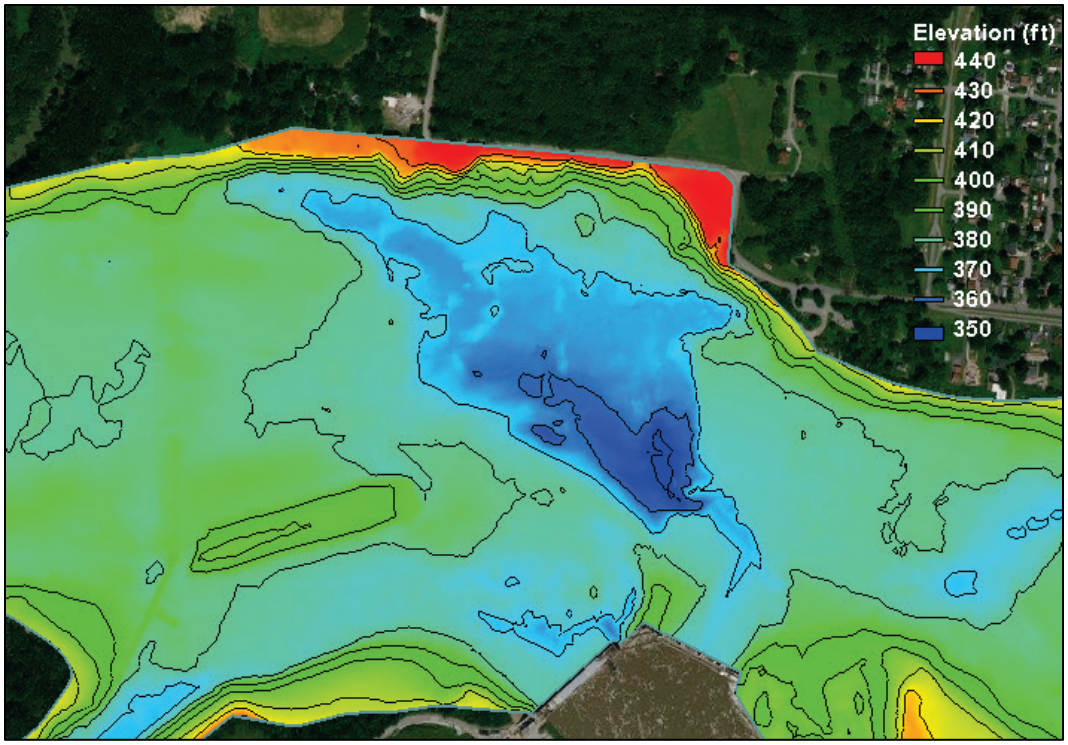

Figure 47. Plan 1 geometry.

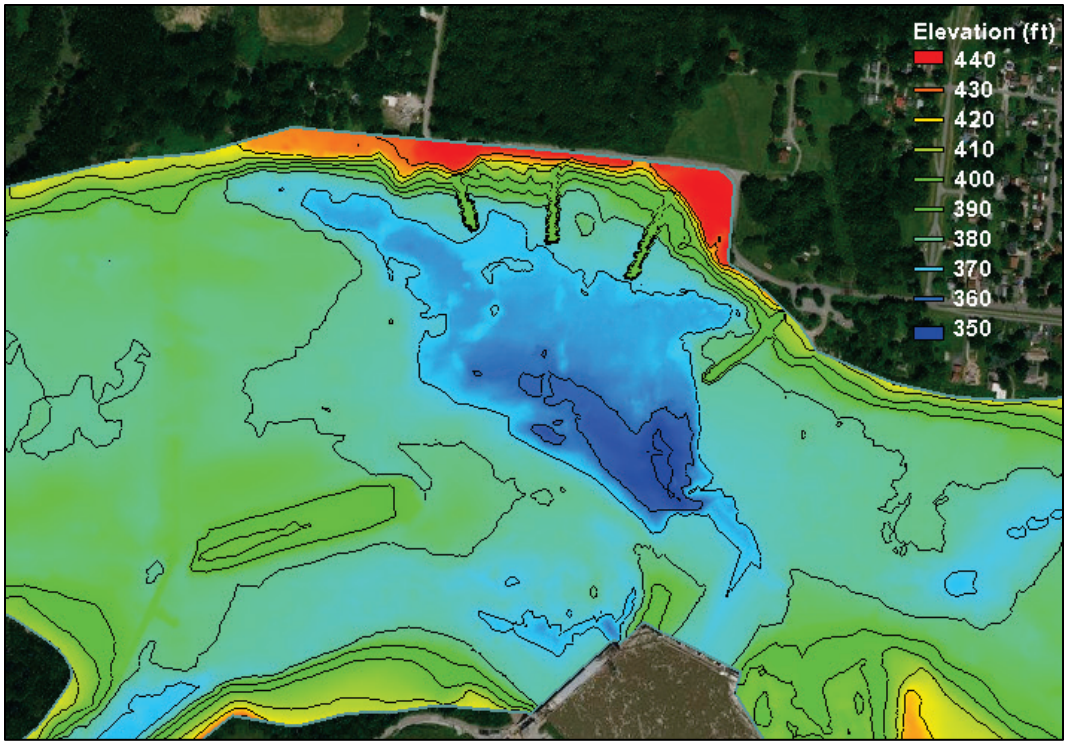

Figure 48. Plan 2 geometry.

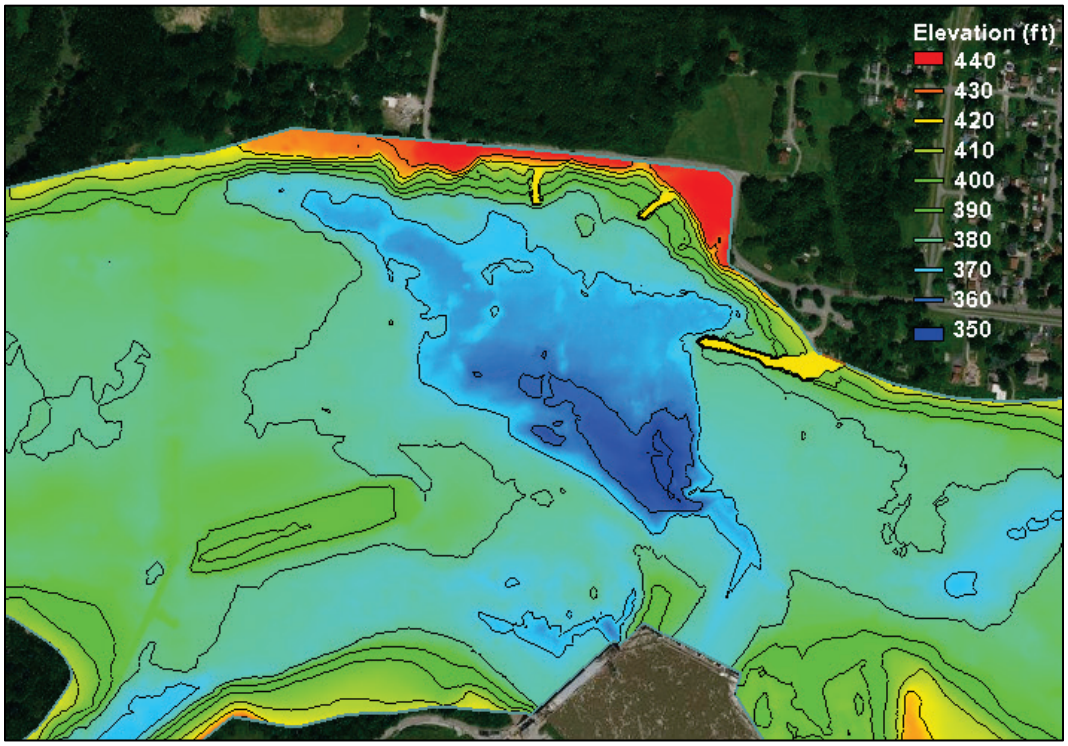

Figure 49. Plan 3 geometry.

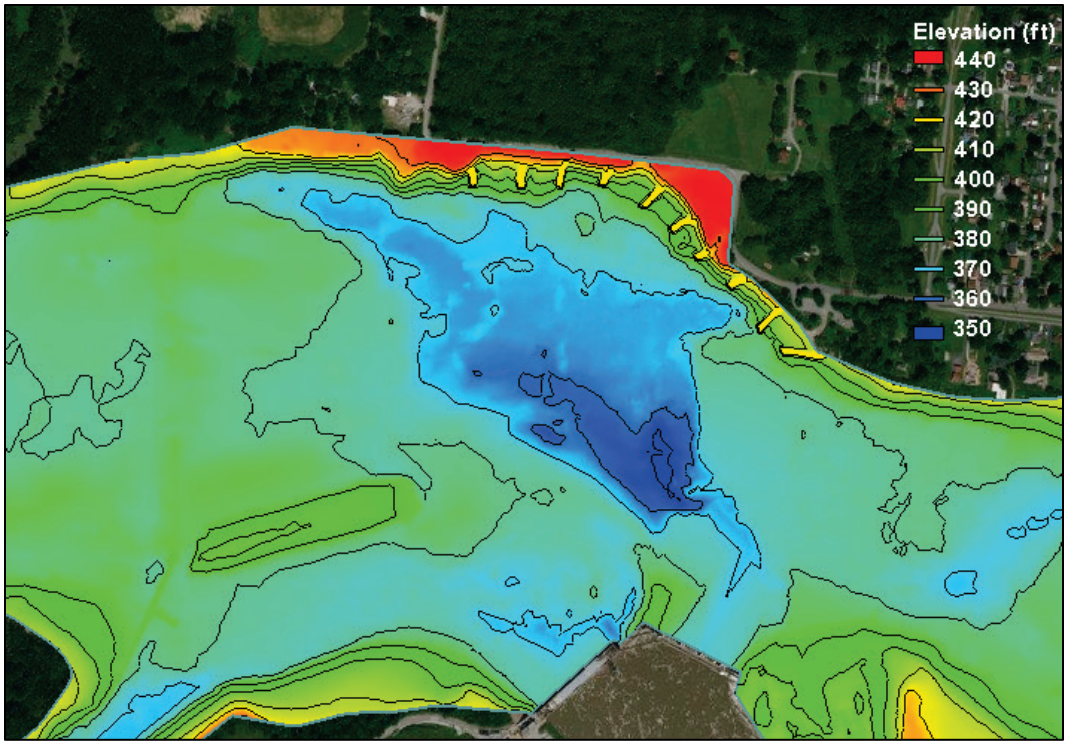

Figure 50. Plan 4 geometry.

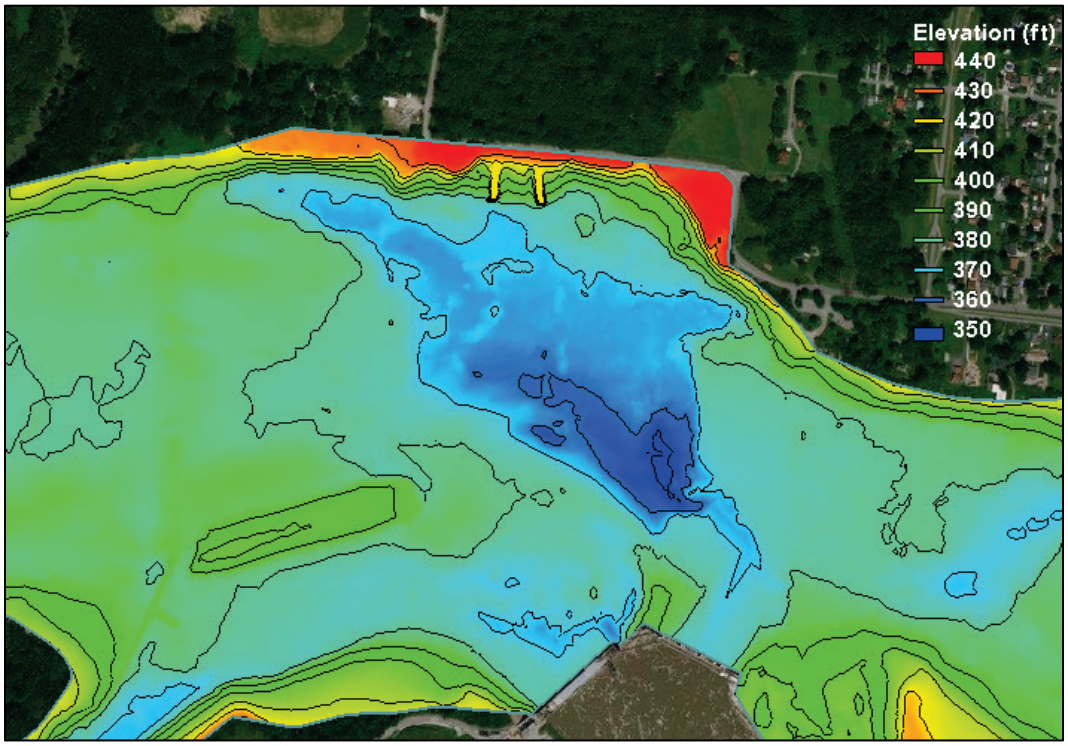

Figure 51. Plan 5 geometry.

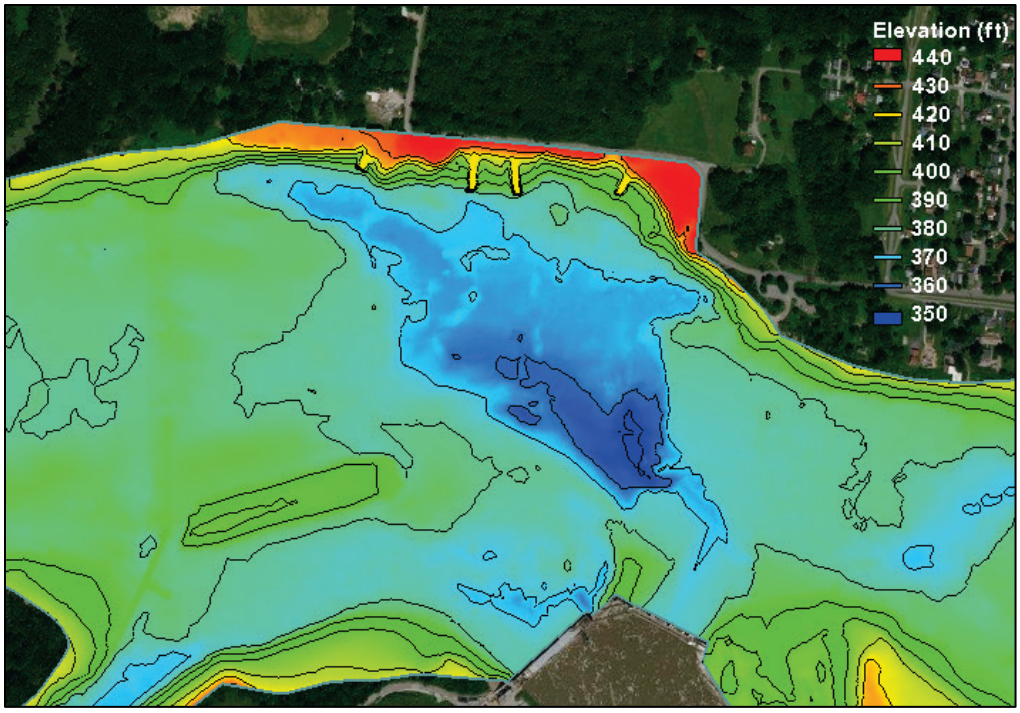

All plans were first tested using the high-flow condition (328 kcfs) with 40% through the upper gates and 60 % through the lower gates. Velocity magnitudes and directions are plotted for the existing condition (no structures) and all five plans for this flow scenario in Figure 52–Figure 57.

Figure 52. Existing velocities 40% upper – 60% lower.

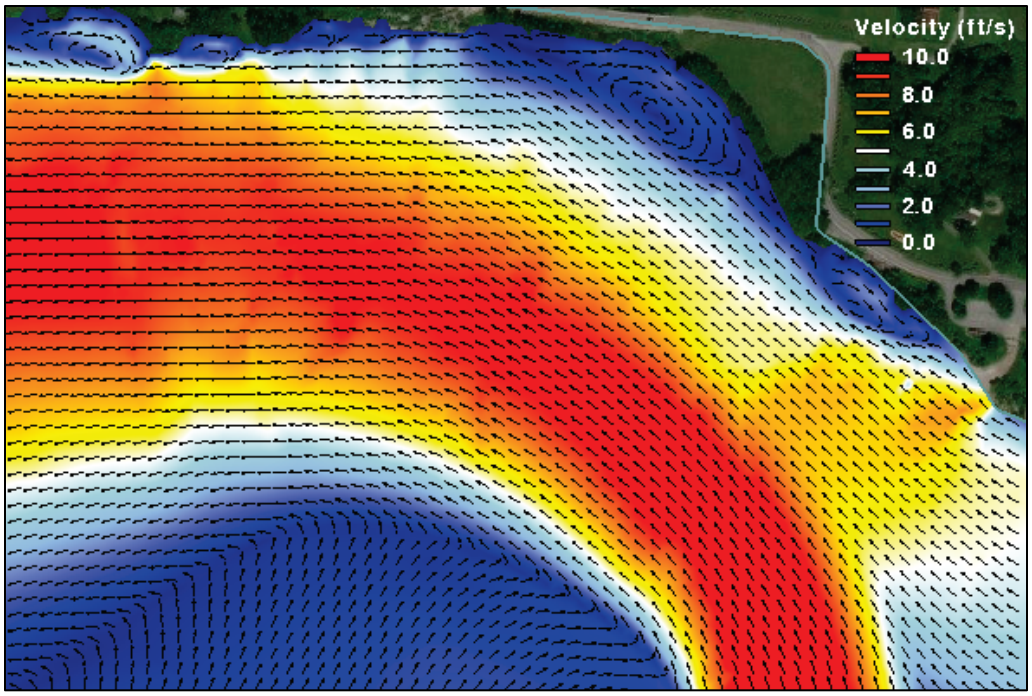

Figure 53. Plan 1 velocities 40% upper – 60% lower.

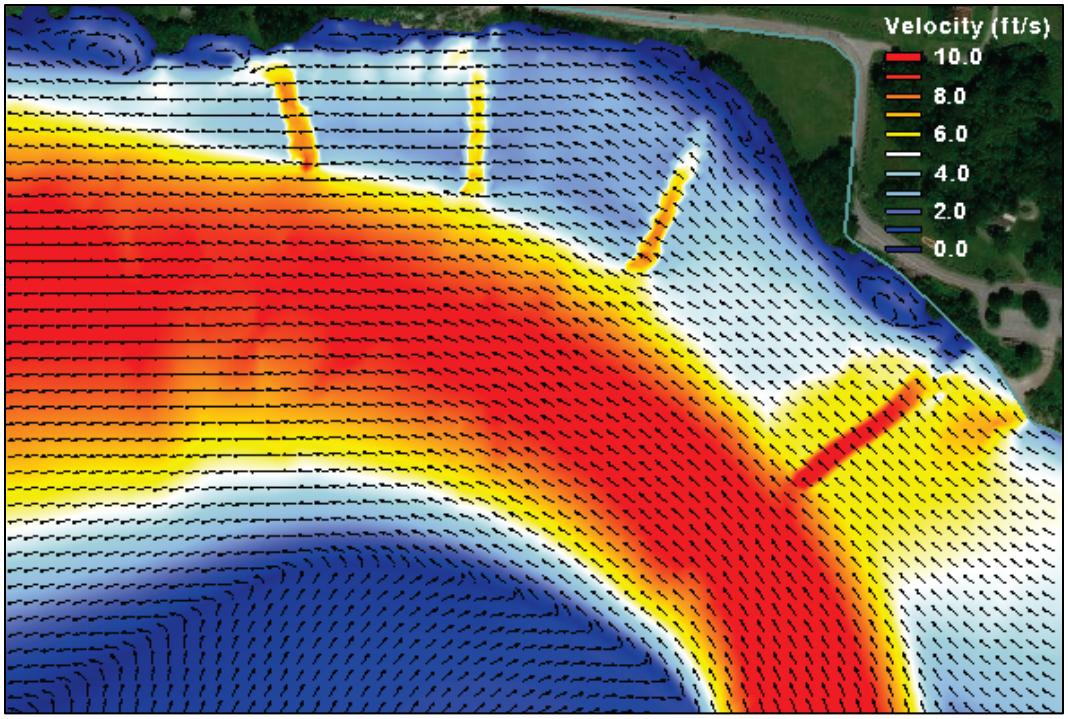

Figure 54. Plan 2 velocities 40% upper – 60% lower.

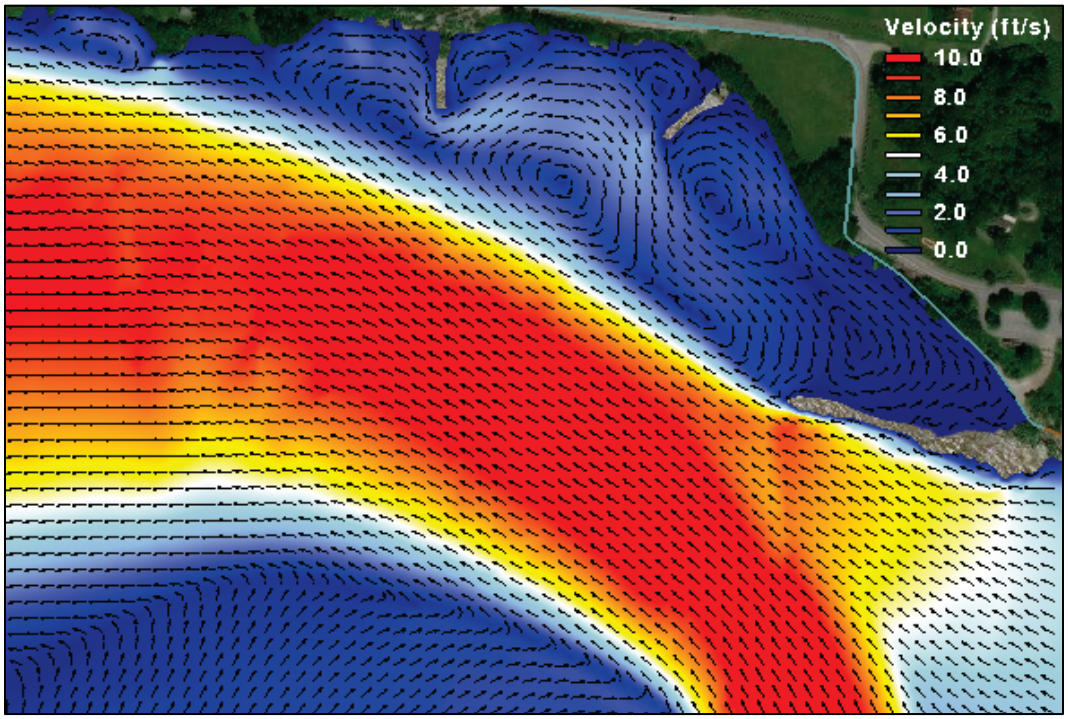

Figure 55. Plan 3 velocities 40% upper – 60% lower.

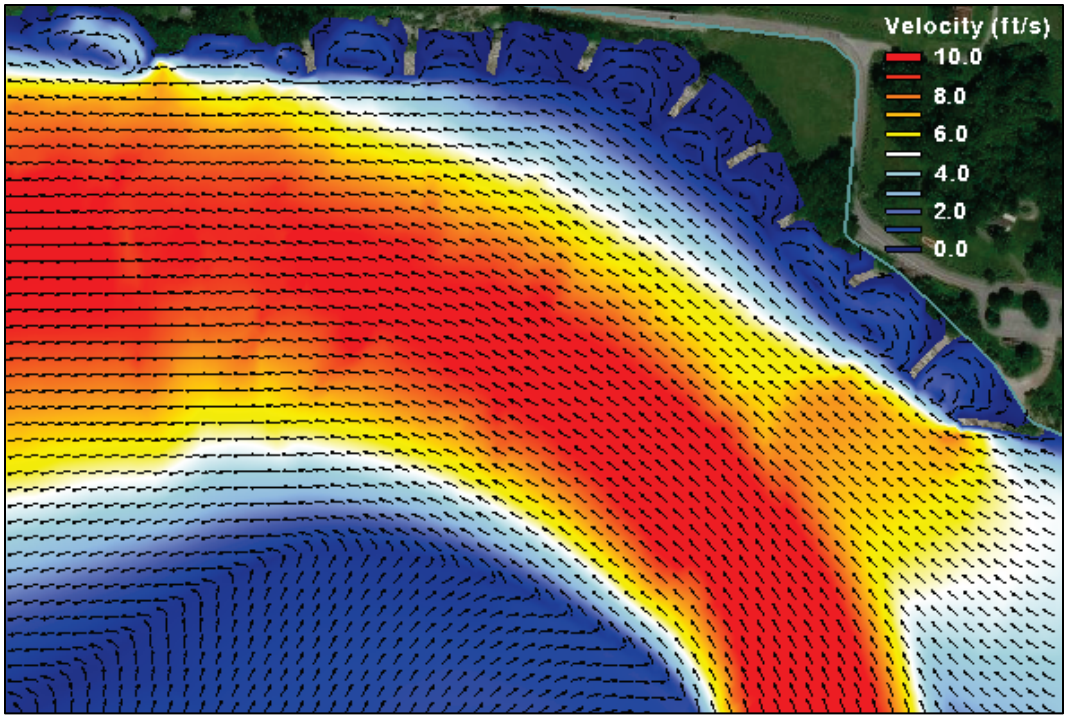

Figure 56. Plan 4 velocities 40% upper – 60% lower.

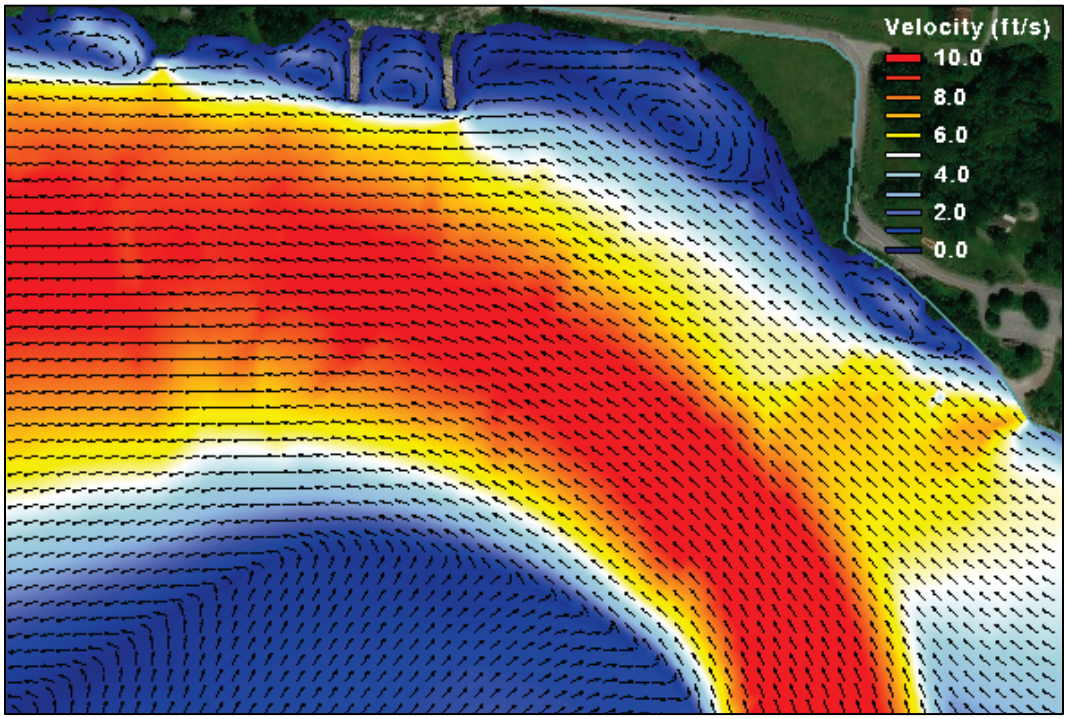

Figure 57. Plan 5 velocities 40% upper – 60% lower.

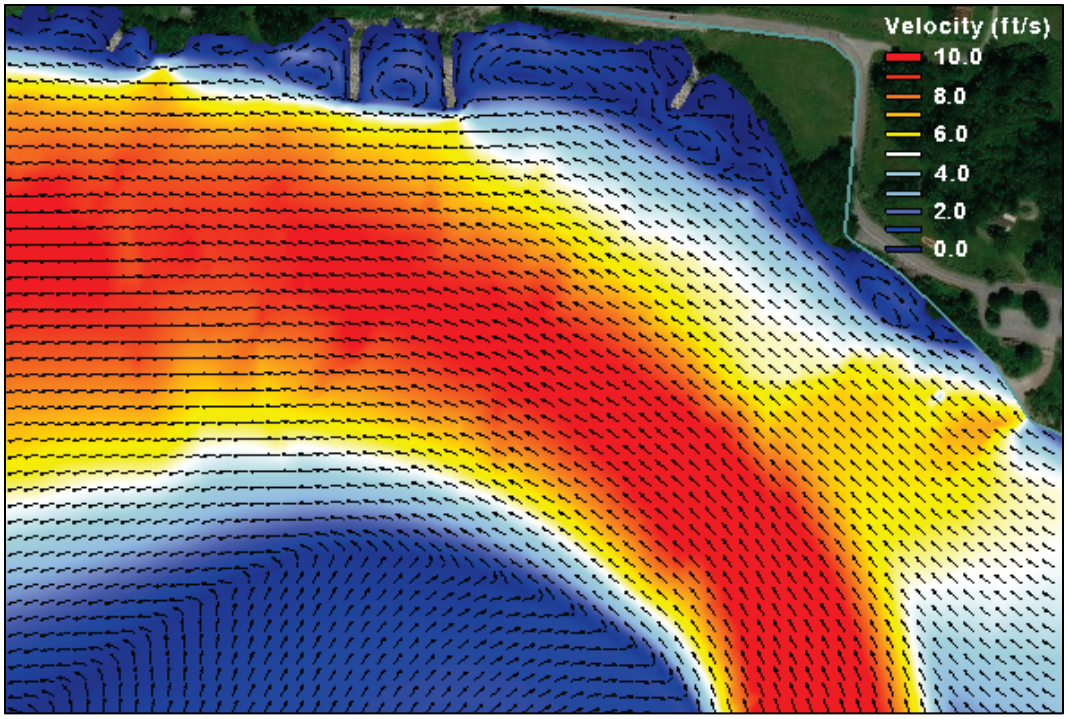

The 60% through upper gates and 40% through lower gates combination was also simulated for all plans to help bracket the velocities. The resulting velocities are plotted for each plan in Figure 58–Figure 63.

Figure 58. Existing conditions velocities 60% upper – 40% lower.

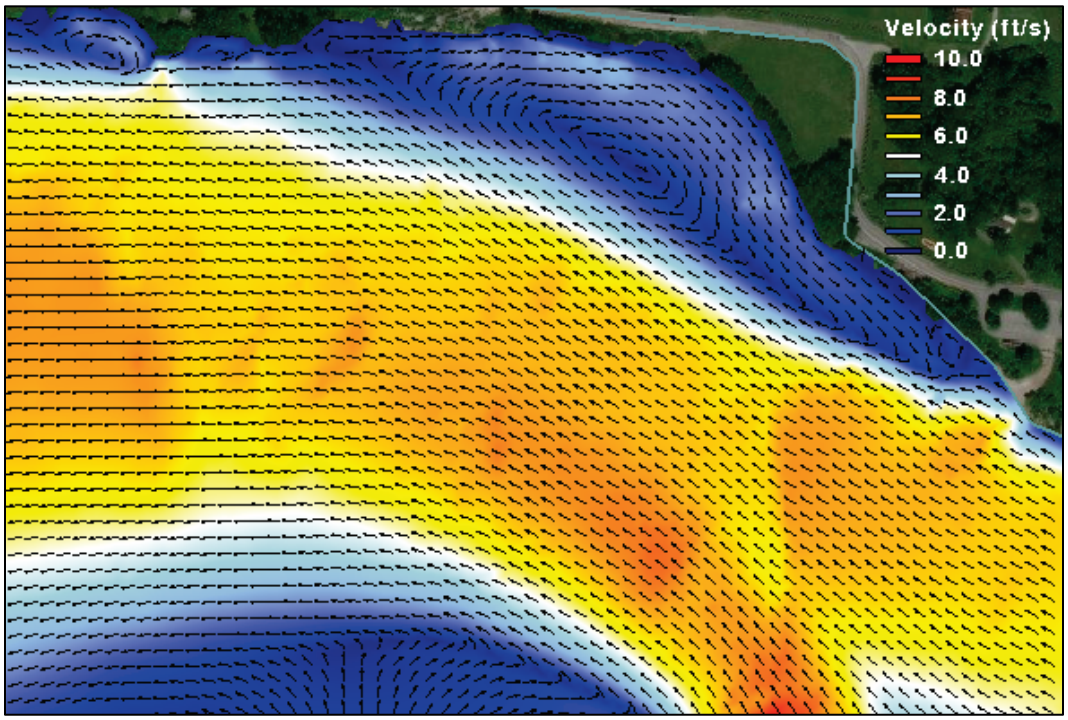

Figure 59. Plan 1 velocities 60% upper – 40% lower.

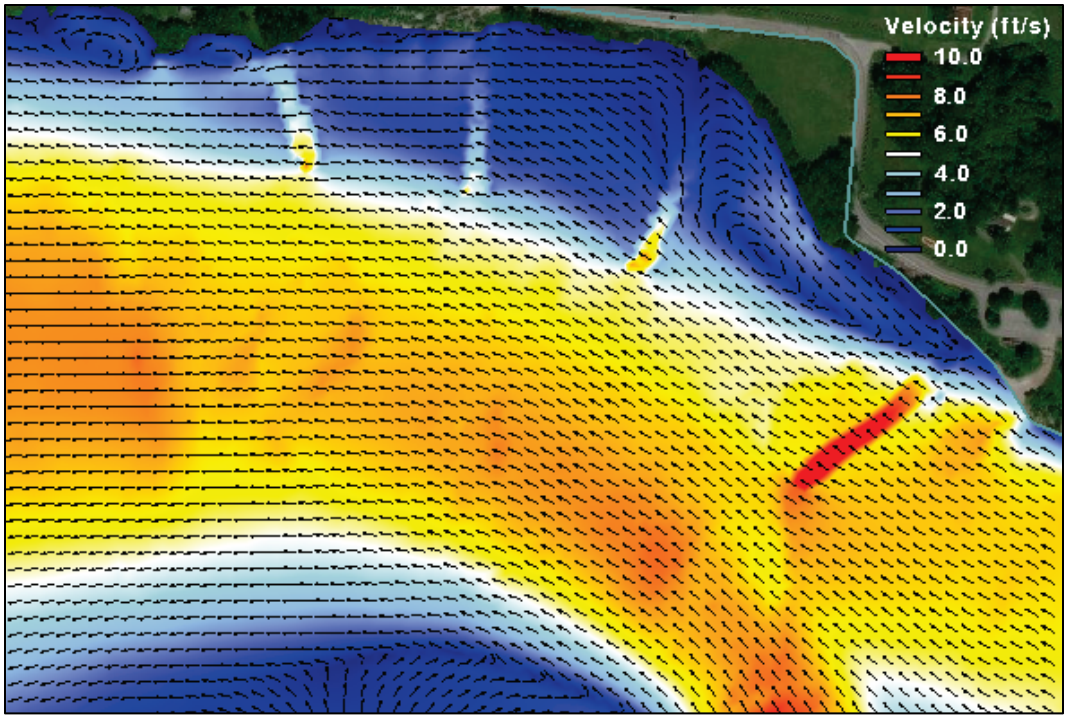

Figure 60. Plan 2 velocities 60% upper – 40% lower.

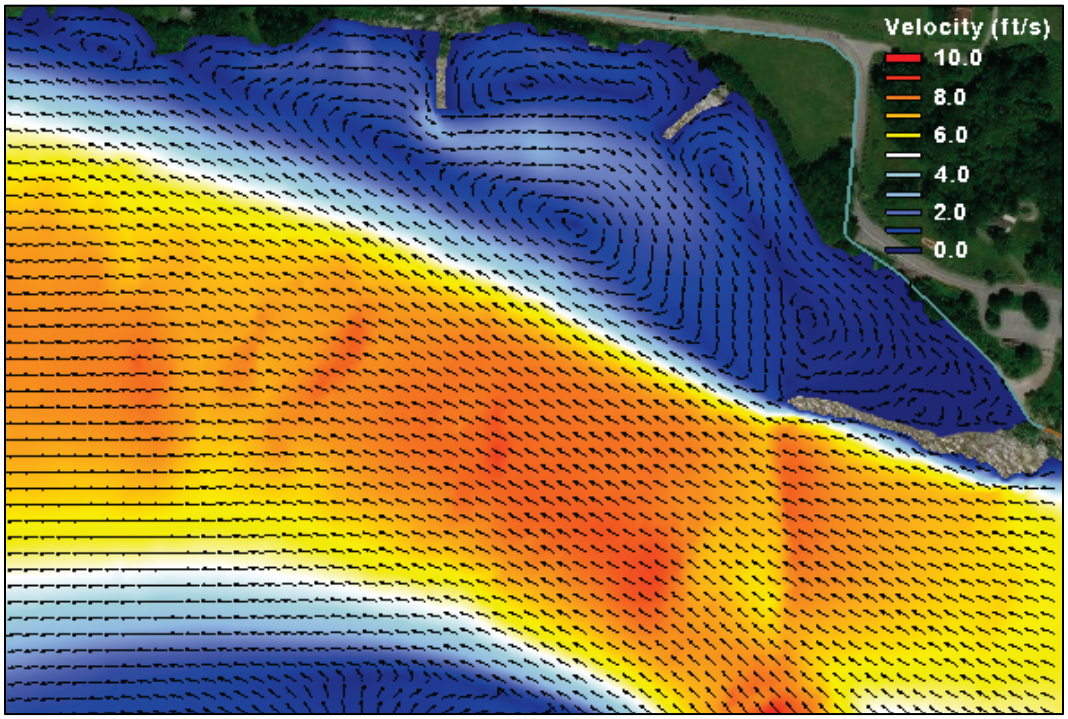

Figure 61. Plan 3 velocities 60% upper – 40% lower.

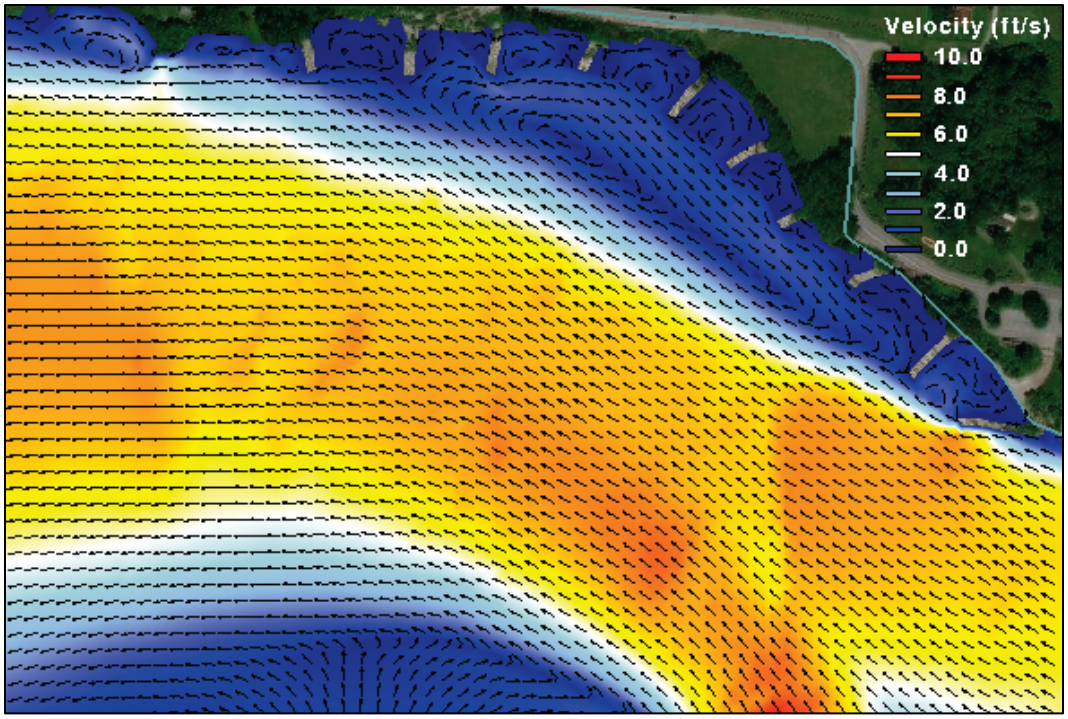

Figure 62. Plan 4 velocities 60% upper – 40% lower.

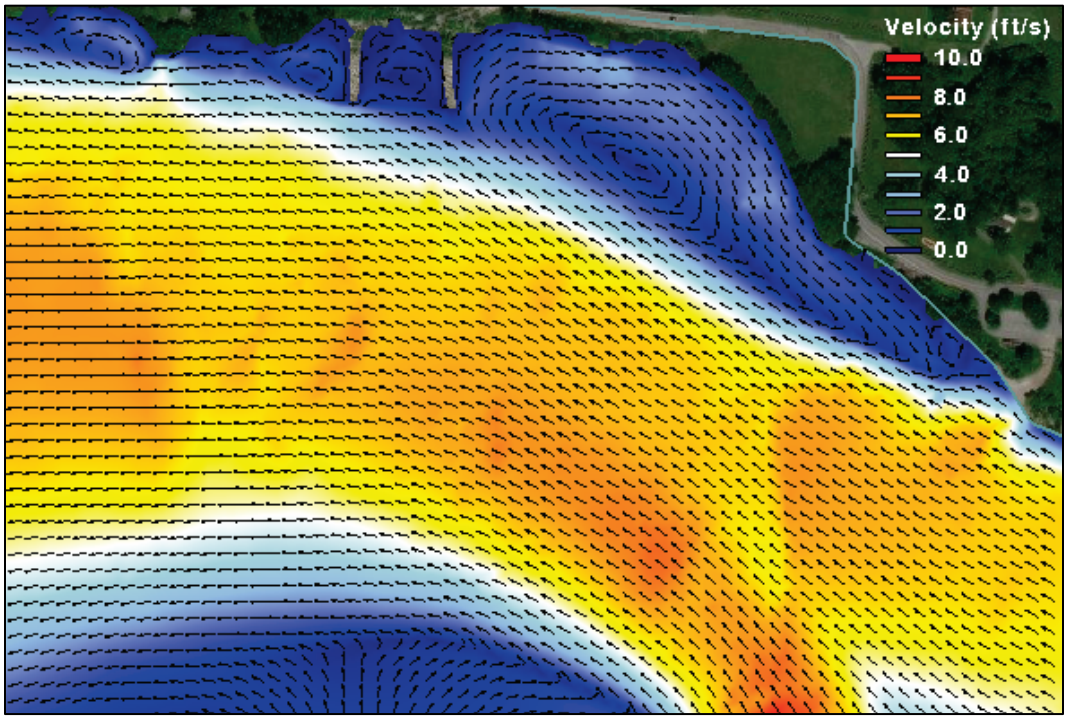

Figure 63. Plan 5 velocities 60% upper – 40% lower.

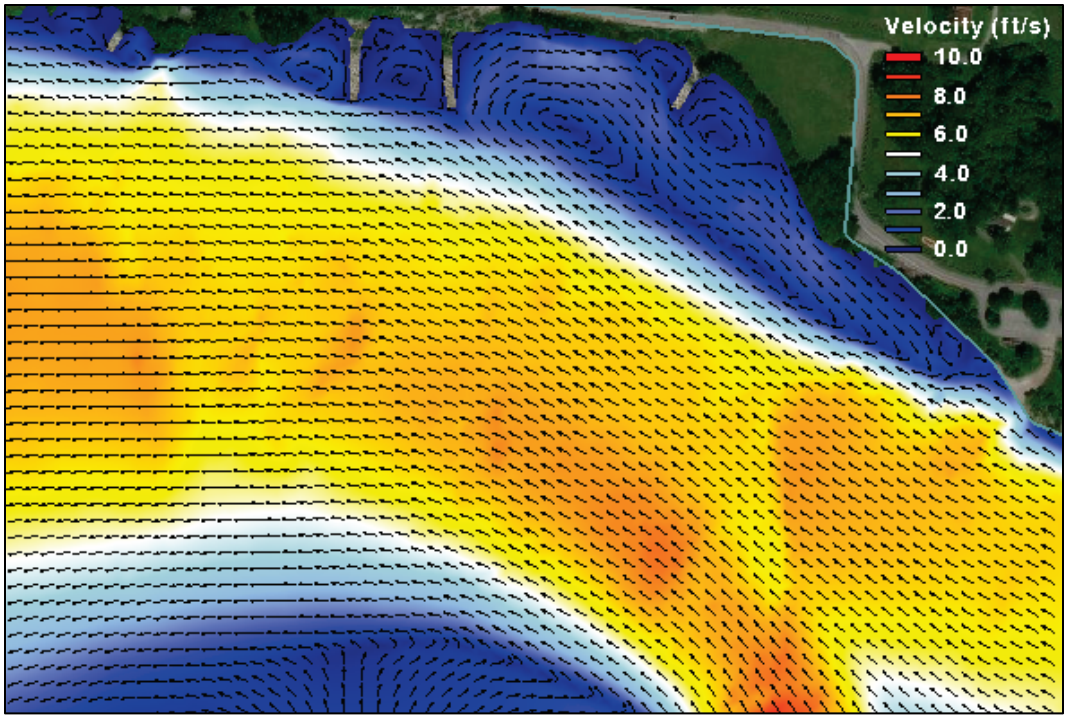

- The goal of Plan 1 is to use submerged weirs to help turn the flow away from the bank. These structures are able to redirect the highest velocities farther into the channel away from the bank. However, the velocities near the bankline are not sufficiently reduced.
- The intent of Plan 2 is to use a large emergent flow deflector to route the velocities away from the bank. The flow deflector is effective in rerouting the highest velocities into the center of the channel, but flow separation occurs behind the structure, and a large high-velocity eddy forms. Two dikes were then added in an effort to break up the circulation behind the flow deflector. These dikes do help to reduce the velocities, but the dike spacing still allows eddies to form between the dikes.
- Plan 3 consists of a system of small dikes with the upstream-most dike angled to act as a small flow deflector. This system is very effective in helping to reduce the velocities on the bank line. The small spacing does not allow much circulation to form between the dikes, thus maintaining low energy between the dikes at the shore line.
- Plan 4 uses two parallel dikes placed in the area where the highest velocities occur for the existing conditions, which coincides with where failure and repair have occurred in the past. These dikes reduce the velocities in that area but do not address other areas where circulation occurs.

- Plan 5 builds on Plan 4 by providing two additional smaller dikes to break up some of the eddy circulation. This combination results in reduced circulation.

6 Discussion

To better determine how the conditions on the eroding bank have changed since construction of the lock and dam system, more data on pre-construction conditions would be needed. Without this, quantitatively defining the impact of the lock and dam since construction is not possible. However, for the present lock and dam configuration the flow patterns for the scenarios tested in this study indicate strong erosion potential in the area of concern. The worst-case scenario was found to be higher flow conditions that do not allow for operational changes as both sets of gates are needed to pass the incoming flow. Therefore, it is recommended that a structural alternative of bank protection or river training structures be considered. Plans 3 and 5 are the most effective at reducing velocities. Both plans consist of smaller dikes placed along the banks. The spacing and location of the dikes are critical factors in whether or not higher velocity circulation occurs between the structures. According to the results of this study, either of these plans or a similar combination could reduce the churning of water that erodes away loose material from the bank at higher flows.

Currently, during low water periods, flow through the upper gates of the project is cut off as much as possible to allow for recreational and educational visits to the fossil fields below the upper gates. Such was the case on 1 July 2007 (Figure 27) when all observed flow through the lower gates was heading directly into the opposite bank of the river. It is evident that these conditions are severe, but the analysis in this report shows that these conditions are not nearly as severe as higher flow conditions through this reach. However, the low-flow simulations (Figure 28 and Figure 29) show that these conditions can still be improved by redistributing some flow through the upper gates. Sufficient flow can be released through the upper gates to redirect velocities in the problem area while still maintaining similar extents and depths in the educational and recreational sites. The depth and lateral extents of the land and water interface for 0% and 20% flow through the upper gates are shown in Figures 64–65. Profiles for 10% increments in flow through the upper gates from 0% to 40% are plotted in Figure 66, which clearly illustrates the increase in depth for each increment in flow.

Figure 64. Depths and extents of flow with 0% flow through upper gates.

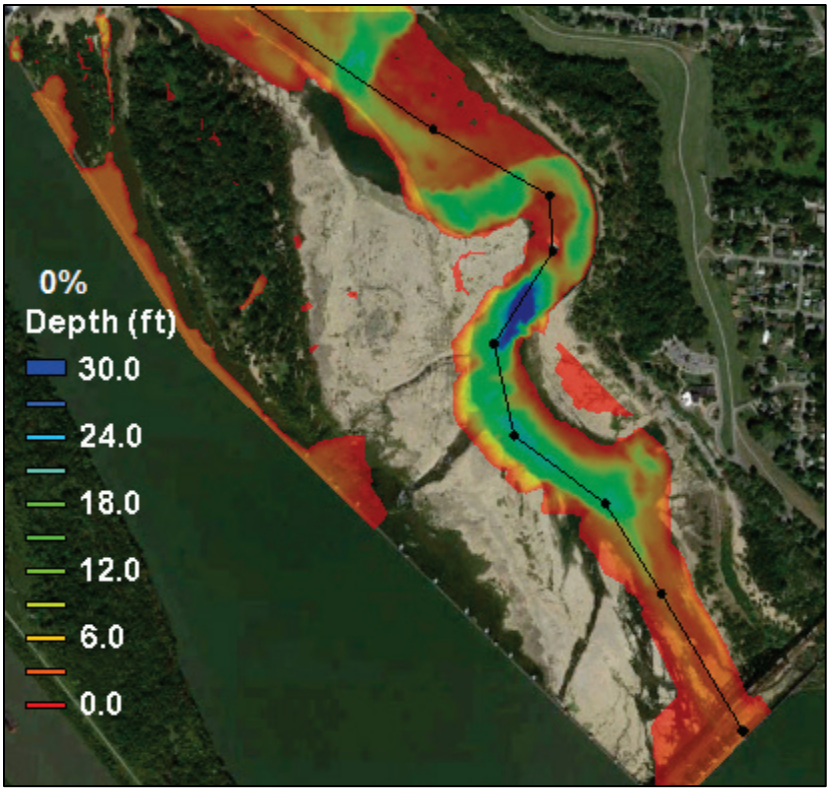

Figure 65. Depths and extents of flow increase with 20% flow through upper gates.

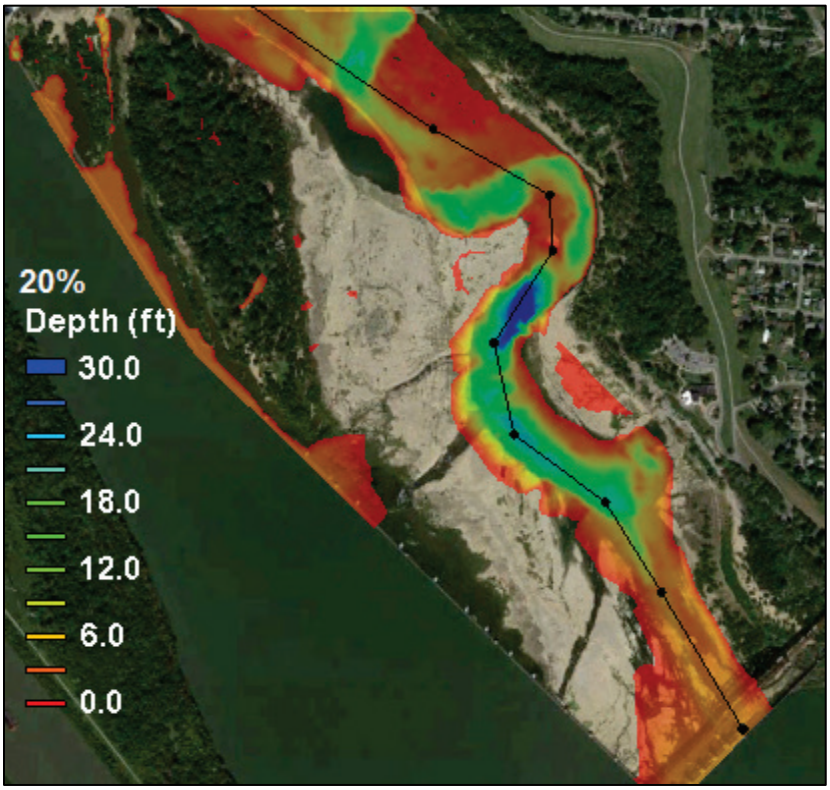

Figure 66. Water surface profiles for 0%, 10%, 20%, 30%, and 40% of low flow through upstream gates.

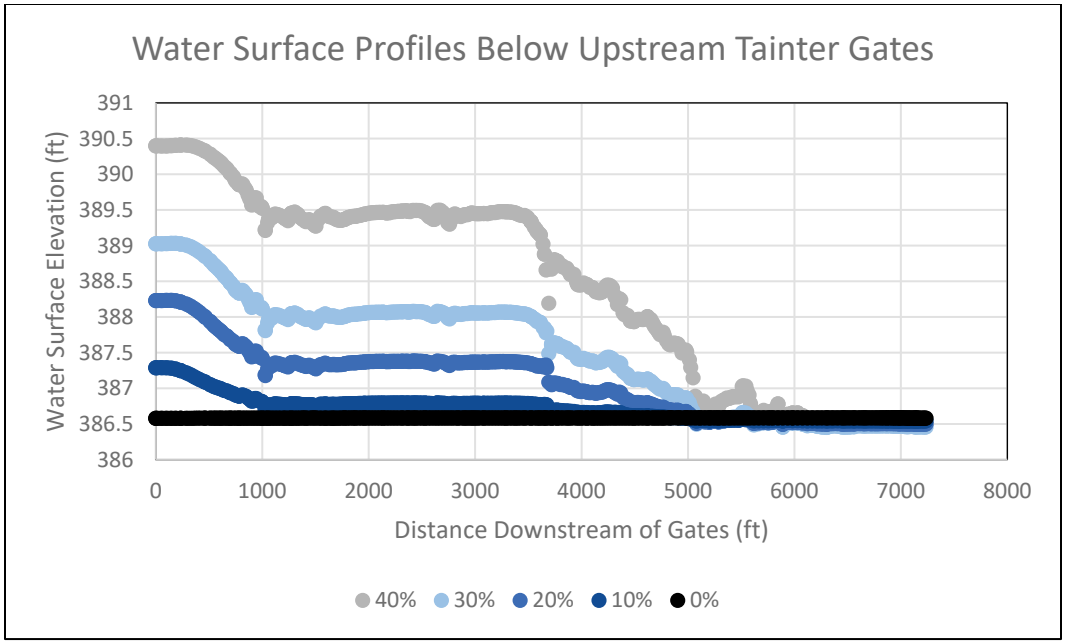

The accessibility of the fossil fields was not the original focus area of this study, so the confidence in this area is reduced due to decreased resolution and an initial lowering of the bathymetry elevation immediately downstream of the gates. This lowering of the bathymetry was done to ensure that the inflow boundary remained wet, which is required to input flow and to prevent supercritical flow directly at the boundary which would decrease model stability and greatly increase computational time as much smaller time steps would be needed. However, the general trends and relative changes are still useful. A small amount of flow through these upstream gates will not significantly change the extents of the water as seen in Figures 64 and 65. The water surface profiles in Figure 66 show that the largest depth increase occurs just downstream of the gates.

7 Conclusions and Recommendations

Gate operations at McAlpine Lock and Dam have a significant impact on flow velocities within the study area. The impact is evident by how much the velocity magnitudes and directions vary when changing the percentage of total flow released through each set of gates. The change is driven by the fact that the lower gates release flow that is normal to the direction of flow in the main channel. Historical images have captured situations, such as the 1 July 2007 flow that was analyzed as the "Low Flow," where all the flow is released through the lower gates and appears to head directly into the opposite bank. Similar low-flow conditions were considered to be one of the worst scenarios as far as flow impingement prior to model simulations. However, the model results indicate much higher velocities occurring during the normal operation of a higher flow. Although the flow does not head directly into the bank, the higher magnitude flow results in higher velocities including some high-velocity eddy circulations that form very close to the edge of the bank. The simulated higher flow conditions were determined to be the worst-case scenario and a better baseline to test the ability of potential structural alternatives to reduce the velocities near the shore.

This study evaluated five plans' effects on velocity patterns. Plans 3 and 5, both composed of multiple small dikes, result in the best reduction of problematic velocities in the area of concern. Model results for these two plans indicate that in-channel structures could have a beneficial impact towards reducing the bank erosion problem. Additionally, dam operational changes during low flow, including never completely cutting off flow from the upstream gates, will help reduce flow velocities on the bank in the problem area. High-flow conditions are likely when the majority of bank erosion occurs, and there is no operational flexibility during these flows. Therefore, it is recommended that river training structures and/or some form of bank protection are needed to protect the bank from future erosion in the problem area.

The calibrated model developed for this study can be used to test additional potential structures or operational procedures. This study focused on determining a baseline condition against which to test the structural alternatives and then testing the structures to see if similar alternatives would be feasible. Further testing could be conducted to determine plan performance in multiple flow conditions.

References

Egiazaroff, I. V. 1965. "Calculation of Non-Uniform Sediment Concentration." *Journal of Hydraulics Division, ASCE* 91(HY4): 225–248.

Meyer-Peter, E., and R. Müller. 1948. "Formulas for Bed-Load Transport." In *Proc., 2nd Meeting, IAHR*. Stockholm, Sweden, 39–64.

U.S. Army Corps of Engineers (USACE). 2015. *Ohio River Shoreline, McAlpine Locks and Dam Caving Bank Condition, Clarksville, Indiana Followup Assessment Report*. Louisville, KY: U.S. Army Corps of Engineers, Louisville District.

U.S. Army Engineer Research and Development Center, Coastal and Hydraulics Laboratory (ERDC CHL), 2017. *Adaptive Hydraulics 2D Shallow Water (AdH-SW2D) User Manual (Version 4.6)*. Vicksburg, MS: U.S. Army Engineer Research and Development Center. https://chl.erdc.dren.mil/adh/documentation/AdH_Manual_Hydrodynamic-Version4.6.pdf.

Wong, M., and G. Parker. 2006. "Reanalysis and Correction of Bed-Load Relation of Meyer-Peter and Müller Using Their Own Database." *Journal of Hydraulic Engineering* 132(11): 1159–1168.

Wright, S., and G. Parker. 2004. "Flow Resistance and Suspended Load in Sand-Bed Rivers: Simplified Stratification Model." *Journal of Hydraulic Engineering* 130(8): 796–805.

REPORT DOCUMENTATION PAGE

Form Approved
OMB No. 0704-0188

1. REPORT DATE	2. REPORT TYPE	3. DATES COVERED *(From - To)*
April 2018	**Final Report**	

4. TITLE AND SUBTITLE
Silver Creek: A Study of Stream Velocities and Erosion along the Ohio River near Clarksville, Indiana; McAlpine Lock and Dam Numerical Model

5a. CONTRACT NUMBER

5b. GRANT NUMBER

5c. PROGRAM ELEMENT NUMBER

6. AUTHOR(S)
Keaton E. Jones, David D. Abraham, Gary L. Bell, and Nate D. Clifton

5d. PROJECT NUMBER
455010

5e. TASK NUMBER

5f. WORK UNIT NUMBER

7. PERFORMING ORGANIZATION NAME(S) AND ADDRESS(ES) (see reverse)
Coastal and Hydraulics Laboratory
U.S. Army Engineer Research and Development Center
3909 Halls Ferry Rd
Vicksburg, MS 39180-6199

8. PERFORMING ORGANIZATION REPORT NUMBER
ERDC/CHL TR-18-4

9. SPONSORING/MONITORING AGENCY NAME(S) AND ADDRESS(ES)
U.S. Army Corps of Engineers, Louisville District
Mazzoli Federal Building
600 Dr. Martin Luther King Jr. Place
Louisville, KY 40201-0059

10. SPONSOR/MONITOR'S ACRONYM(S)
USACE LRL

11. SPONSOR/MONITOR'S REPORT NUMBER(S)

12. DISTRIBUTION/AVAILABILITY STATEMENT
Approved for public release; distribution is unlimited.

13. SUPPLEMENTARY NOTES

14. ABSTRACT

The River Engineering Branch of the Coastal and Hydraulics Laboratory conducted a two-dimensional numerical model investigation of the Ohio River immediately downstream of McAlpine Lock and Dam. The right bank between river mile 605.5 and 606.5 (opposite the dam's downstream set of tainter gates) has historically experienced stability issues. Conditions on the bank, when observed through aerial imagery, appear most severe when the dam is releasing all or most flow through the downstream (lower) set of tainter gates. Releasing all flow through the downstream gates occurs only at lower flow rates, but this study determined that standard high-flow conditions create higher velocities in the problem area than these observed low-flow conditions. The representative high-flow event was then used to test the capability of structural alternatives to reduce velocities in the area of concern. Plans consisting of small emergent dikes placed along the shoreline were able to reduce the velocities significantly and could be a feasible alternative to help protect the bankline.

15. SUBJECT TERMS

Hydraulic structures, McAlpine Locks and Dam (Ky.)—Environmental aspects, sedimentation and deposition—Ohio River, Soil erosion, Streamflow

16. SECURITY CLASSIFICATION OF:			17. LIMITATION OF ABSTRACT	18. NUMBER OF PAGES	19a. NAME OF RESPONSIBLE PERSON
a. REPORT	b. ABSTRACT	c. THIS PAGE			Gary Bell
Unclassified	Unclassified	Unclassified	SAR	59	**19b. TELEPHONE NUMBER** *(Include area code)* 601-634-4621